Journal of Medicinal Chemistry

ARTICLE

pubs.acs.org/jmc

Development of Tetrahydroisoquinoline-Based Hydroxamic Acid Derivatives: Potent Histone Deacetylase Inhibitors with Marked in Vitro and in Vivo Antitumor Activities

Yingjie Zhang,[†] Jinhong Feng,[†] Yuping Jia,[†] Xuejian Wang,[†] Lei Zhang,[†] Chunxi Liu,[§] Hao Fang,*[,†] and Wenfang Xu*[,†]

Departments of [†]Medicinal Chemistry and [§]Pharmaceutics, School of Pharmacy, Shandong University, Ji'nan, Shandong, 250012, People's Republic of China

Supporting Information

ABSTRACT: Inhibition of histone deacetylase (HDAC) results in growth arrest, differentiation, and apoptosis in nearly all tumor cell lines, promoting HDACs as promising targets for antitumor therapy. In our previous study we developed a novel series of 1,2,3,4-tetrahydroisoquinoline-3-carboxylic acid derivatives as HDAC inhibitors (HDACi), among which compound **7d** exhibited promising HDAC8 inhibitory and antiproliferative activities. Herein, we report the design and development of a new class of tetrahydroisoquinoline-bearing hydroxamic acid analogues as potential HDACi and anticancer agents. In vitro biological evaluation of these compounds showed improved HDAC8 inhibition (compounds **31a** and **31b** exhibited mid-nM IC_{50} values against HDAC8) and potent growth inhibition in multiple tumor cell lines. Most importantly, compounds **25e**, **34a**, and **34b** exhibited excellent in vivo anticancer activities in a human breast carcinoma (MDA-MB-231) xenograft model compared with suberoylanilide hydroxamic acid (SAHA), an approved HDACi. Collectively, our results indicate that tetrahydroisoquinoline bearing a hydroxamic acid is an excellent template to develop novel HDACi as potential anticancer agents.

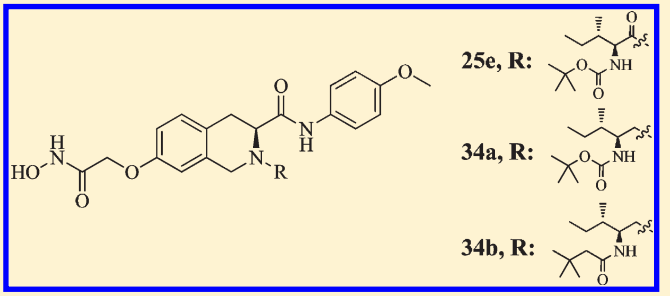

INTRODUCTION

Histone deacetylases (HDACs[α]) are enzymes that catalyze the deacetylation of lysine residues located at the N-terminus of various protein substrates, such as nucleosomal histiones. The hydrolysis of the acetyl group from histones results in condensed chromosomal DNA and transcriptional repression.[1−3] There are 18 human HDACs grouped into 4 classes[4,5] based on their homology to yeast models: classes I (HDACs 1−3 and 8), II (HDACs 4−7, 9, and 10), and IV (HDAC 11) are zinc-dependent metallohydrolases, namely "classical HDACs",[4] whereas class III HDACs (sirtuins 1−7) are NAD^+ dependent.[6] All the zinc-dependent HDACs bear a highly conserved catalytic site.

Over the past few years, multiple nonhistone proteins involved in cell growth and survival pathways have been identified as substrates of HDACs, including transcription factors, cytoskeletal proteins, molecular chaperones and nuclear import factors.[7] In this context, dysregulation of HDACs has been linked to the pathogenesis of many diseases, of which cancer is the most intractable. It has been revealed that overexpression of classes I and II HDACs, especially class I isozymes, is associated with various human cancers.[8−15] Therefore, there has been a high level of interest in developing HDAC inhibitors (HDACi), and numerous structurally diverse HDACi have been developed as potential anticancer agents (Figure 1).[16] As shown in Figure 1, the common pharmacophore of these HDACi consists of three domains: a zinc-binding group (ZBG), such as hydroxamic acid; a cap group, generally a hydrophobic and aromatic group; a saturated or unsaturated linker domain, composed of linear or cyclic structures that connect the ZBG and the cap group.

Treatment of various transformed cells with HDACi results in significant growth arrest, differentiation, and apoptosis.[17−19] Up to now, two HDACi, suberoylanilide hydroxamic acid (**1**, SAHA, Vorinostat)[20,21] and the depsipeptide FK228 (**2**, Romidepsin),[22] have been approved by the US Food and Drug Administration (FDA) for the treatment of cutaneous T-cell lymphoma (CTCL), validating HDACs' potential as an important target for anticancer therapy. Other HDACi in clinical trials include hydroxamic acids, such as panobinostat (**3**, LBH-589), belinostat (**4**, PXD101), givinostat (**5**, ITF-2357), SB-939 (**6**), R306465 (**7**), and CRA024781 (**8**), benzamides, such as entinostat (**9**, MS-275), mocetinostat (**10**, MGCD-0103), and tacedinaline (**11**, CI-994), and aliphatic acids, such as valproic acid (**12**), sodium phenylbutyrate (**13**), and pivanex (**14**, AN-9).[23]

Recently, we have embarked on the development of tetrahydroisoquinoline-based hydroxamic acid as a novel HDACi scaffold.[24] Biological evaluation showed that HDACi with rigid

Received: December 17, 2010
Published: April 05, 2011

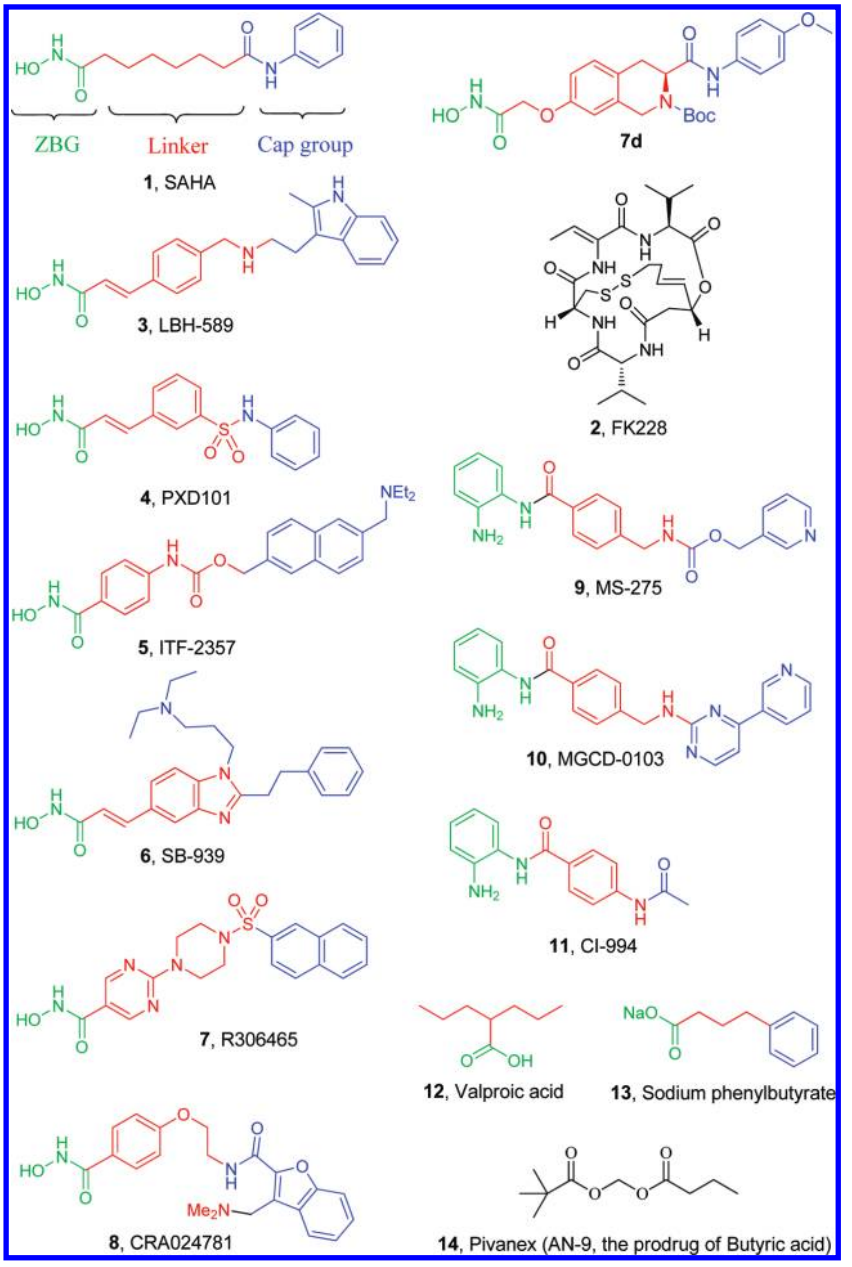

Figure 1. Pharmacophore model and structures of representative HDACi.

tetrahydroisoquinoline scaffold as the linker domain have comparable activities as SAHA (e.g., compound **7d**, Figure 1). In the present study, we report the design, synthesis, and biological characterization of a new series of tetrahydroisoquinoline derivatives based on **7d** to conduct extensive structure−activity relationship (SAR) studies and to optimize their anticancer activities. The *tert*-butoxycarbonyl-protected isoleucine derivative **25e** and its analogues **34a**, **34b** showed similar, or in some cases even more potent, in vitro and in vivo antitumor activities when compared with SAHA.

RESULTS AND DISCUSSION

Chemistry. We designed a series of tetrahydroisoquinoline derivatives with the general structure shown in Figure 2, based on the structure of lead compound **7d**. Compounds **22a**, **22b**, and **22c** were synthesized using the procedures described in

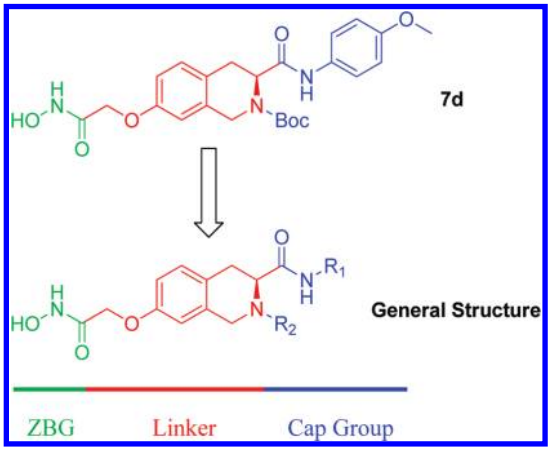

Figure 2. Design idea and a general structure of the target compounds.

dx.doi.org/10.1021/jm101605z |*J. Med. Chem.* 2011, 54, 2823–2838

Scheme 1. Synthesis of Compounds 22a−c[a]

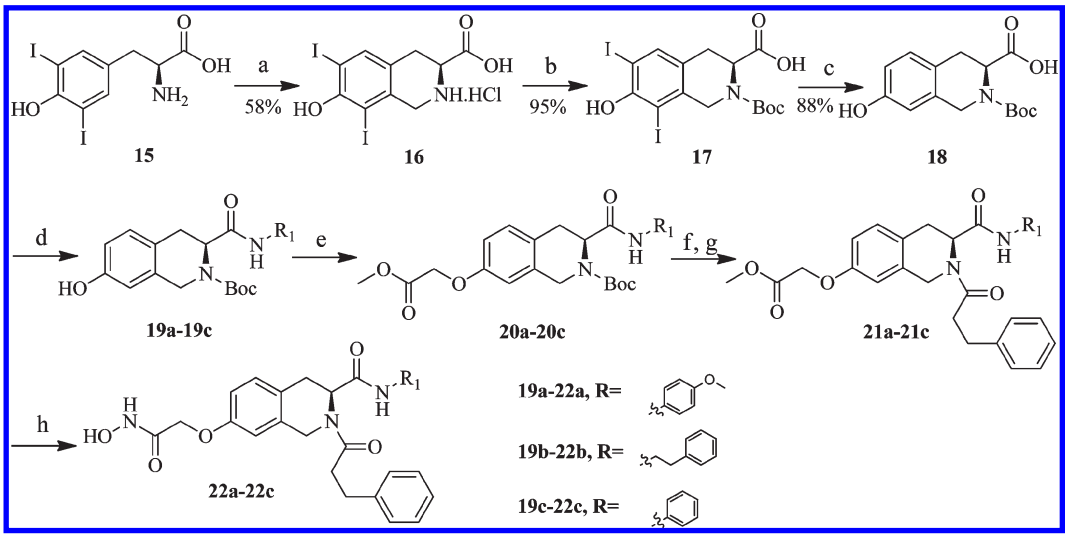

[a] Reagents and conditions: (a) $(CH_2O)_n$, 37% HC1, $CH_3OCH_2CH_2OCH_3$, 72−75 °C, 18 h, 58%; (b) $(Boc)_2O$, 1 N NaOH, THF, 95%; (c) 10% Pd−C, H_2, Et_3N, MeOH, 88%; (d) R_1NH_2, DCC, HOBT, anhydrous THF, 84−91%; (e) $BrCH_2COOCH_3$, K_2CO_3, anhydrous DMF, 61−67%; (f) TFA, Et_3N, DCM, 94−96%; (g) 3-phenylpropionic acid, TBTU, Et_3N, THF, 60−67%; (h) NH_2OK, CH_3OH, 56−59%.

Scheme 1.[24] The tetrahydroisoquinoline ring of **16** was constructed from the starting material 3,5-diiodo-L-tyrosine (**15**) by reaction with formaldehyde. Boc protection and hydrogenolytic removal of the two iodo groups led to **18**. Amidation of **18** followed by phenol hydroxyl group alkylation with bromoacetate gave **20**. Subsequent N-deprotection of **20a−c** with trifluoroacetic acid and condensation with 3-phenylpropionic acid afforded compounds **21a−c**. The ester groups of **21a−c** were treated with NH_2OK in methanol to get target compounds **22a−c**.

N-Deprotection of **20a** with trifluoroacetic acid afforded a key intermediate **23** (Scheme 2). Subsequent derivatization on the secondary amine of **23** under conditions b, c, or d gave compounds **24a−n**, which were treated with NH_2OK in methanol to give compounds **25a−n**. Finally, compounds **26a−h** were achieved by removing the Boc groups of **25a−h** in HCl-saturated ethyl acetate.

Three kinds of dipeptide or dipeptidomimetic **28a−c** were prepared according to the classical peptide synthesis method involving esterification, condensation, and saponification (Scheme 3). Then **28a−c** were installed onto the intermediate **23** to afford compounds **29a−c**, which were finally transformed into target hydroxamate compounds **30a−c** and **31a−c**.

The key steps from amino acid **27** to aldehydes **32a** and **32b** followed reported procedures.[25] Reductive amination of **23** with **32a**, or **32b** using sodium triacetoxyborohydride, followed by ammonolysis of the ester group led to our target compounds **34a** and **34b**, respectively (Scheme 4).

Biological Results. On the basis that all zinc ion-dependent HDACs were highly conserved in their active sites and HDAC8 is more available in our group, first, we still used HDAC8 as the enzyme source to screen our target compounds efficiently. Previously obtained SAR and molecular docking information of compound **7d** and its homologues indicated that the 4-methoxyphenyl group was optimal for the R_1 group, and the R_2 group (for example, *tert*-butoxycarbonyl group in **7d**) was also a significant contributor to HDAC inhibitory activity.[24] In order to further verify this conclusion, we evaluated compounds **22a**, **22b**, and **22c** (Scheme 1). The HDAC8 inhibition assay of these three compounds revealed that **22a** with a 4-methoxyphenyl as the R_1 group was the most potent (Table 1). Besides, as a result of the 3-phenylpropanoyl being the R_2 group, all three compounds possessed a lower IC_{50} than that of **7d**. These results encouraged us to keep the 4-methoxyphenyl group fixed and replace the Boc group of **7d** with other functional groups.

Compounds synthesized in Scheme 2 were specifically designed to probe the effect of the N-substituent. HDAC8 inhibition assay showed that most of these derivatives were more potent than the lead compound **7d**, except **26a**, **26e**, **26g**, **26h**, **25l**, **25m**, and **25n** (Table 2). It was remarkable that compounds with a Boc group (compounds **25a−h**) were more potent than their corresponding deprotected analogues (compounds **26a−h**) without exception. For example, the IC_{50} of compound **25a** was 0.514 μM, much lower than that of compound **26a** (2.14 μM). This indicates that the hydrophobicity of the HDACi cap group is very beneficial to the HDAC inhibitory activity. Compared with their corresponding tertiary amine analogues **25l**, **25m**, and **25n**, compounds **22a**, **25i**, and **25j** were almost 1 order of magnitude more potent, which showed that reduction of the amide group to a tertiary amine group was somewhat detrimental to activity.

To further investigate the antiproliferative activities of these derivatives, several potent compounds were selected to test their effects on the viability of A549 (lung cancer) and MDA-MB-231 (breast cancer) cell lines with SAHA as the positive control. The results presented in Table 3 showed that the antiproliferative activities of these derivatives were similar to that of SAHA. It is remarkable that compound **25e** has an IC_{50} that is 40% lower than that of SAHA against the MDA-MB-231 cell line. Encouraged by its promising in vitro activity, compound **25e** was progressed to an in vivo experiment. Considering that the MDA-MB-231 cell line was to some extent more sensitive to our compounds, especially to **25e**, we established a subcutaneous MDA-MB-231 xenograft model. Because compound **25e** exhibited similar cytotoxicity against normal human fibroblast cells relative to SAHA (data not reported), we compared antitumor

dx.doi.org/10.1021/jm101605z |J. Med. Chem. 2011, 54, 2823–2838

Scheme 2. Synthesis of Compounds 25a−n 26a−h[a]

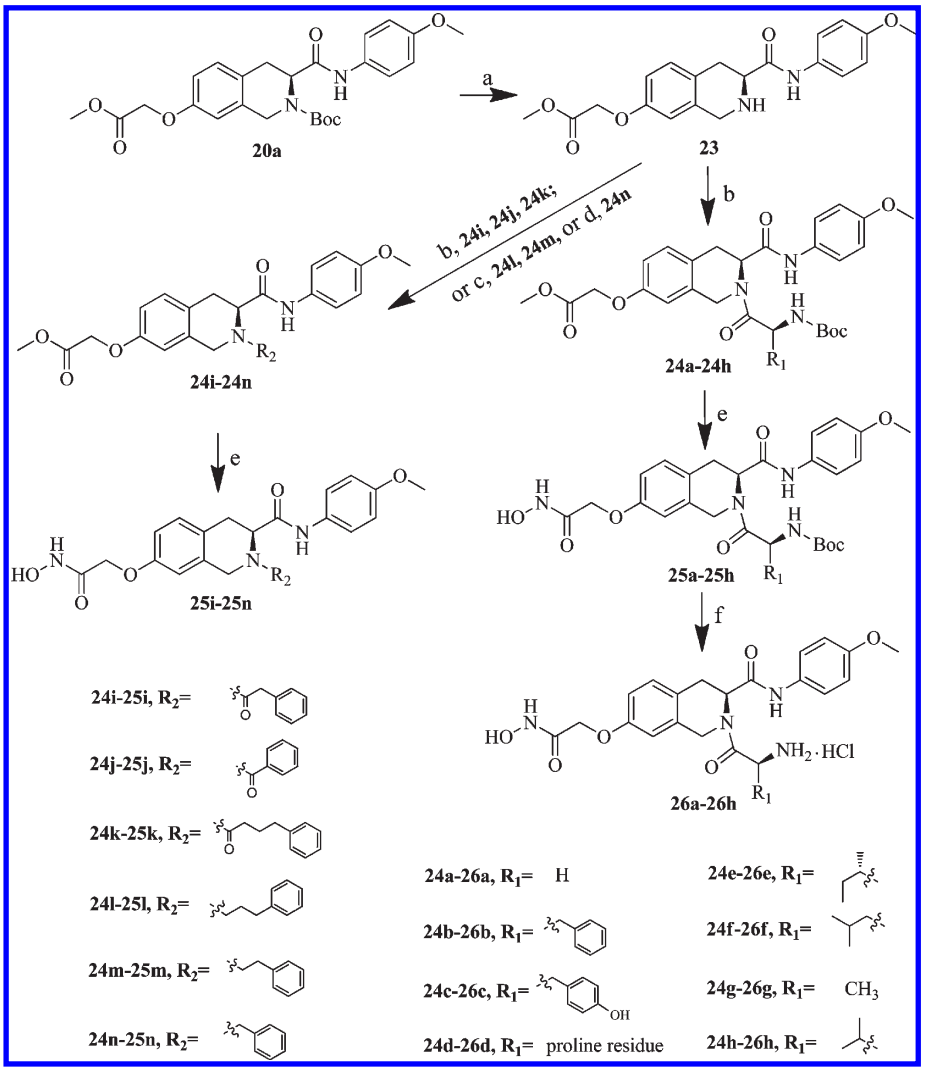

[a] Reagents and conditions: (a) TFA, Et_3N, DCM, 94%; (b) carboxylic acids or Boc-protected amino acids, TBTU, Et_3N, THF, 60−67%; (c) microwave, R_2Br, K_2CO_3, DMF, 75−81%; (d) benzyl bromide, K_2CO_3, DMF, 86%; (e) NH_2OK, CH_3OH, 52−58%; (f) HCl, anhydrous EtOAc, 88−93%.

effects of **25e** and SAHA at the same dosage, 90 mg/kg, which is close to the toxic dosage in mice of SAHA (100 mg/kg).[26] In detail, once tumors became about 100 mm^3, mice were dosed intraperitoneally with either **25e** (90 mg/kg once a day) or SAHA (90 mg/kg once a day) for 21 days. During the treatment, no significant body weight difference among these groups of mice and no signs of evident toxicity were detected. The relative increment ratio (T/C) of **25e** was 63%; meanwhile SAHA was 64%. Both the SAHA-treated group and the **25e**-treated group were significantly different from the control group ($p < 0.05$) by Student's two-tailed t test. As presented in Figure 3, compound **25e** was demonstrated to have in vivo antitumor efficacy comparable to that of SAHA.

Further optimization and modification focused on compound **25e** were conducted. First, to check the role of the Boc group in **25e**, three kinds of dipeptide or dipeptidomimetic residues (**28a**−**c**) were used to substitute the Boc-isoleucine residue of **25e**. These compounds were also tested against HDAC8 and showed similar (**30a**, **30b**, and **30c**) or much higher (**31a**, **31b**) potency relative to **25e** (Table 4). However, further cellular activity evaluation revealed that their antiproliferative activities were not as good as **25e** (Table 5), probably because of less cell membrane permeability compared to **25e**. These results indicated that the geometric confirmation and lipophilicity of the Boc group were beneficial; only minor modification was tolerated in the optimization of **25e**.

Then, compounds **34a** and **34b** were designed and synthesized (Scheme 4). Compared with **25e**, **34a** could have better water solubility in the form of a salt. Considering that the tertiary butyloxycarbonyl group (Boc group) of **34a** was sensitive to acidic conditions and thus might be destroyed by gastric acid, and that the carbamate of **34a** might be metabolized,[27,28] we developed compound **34b**. The enzyme inhibition results in Table 4 are in line with aforementioned SAR in which reduction of the amide group to the tertiary amine group resulted in decreased activity. General in vitro antiproliferative abilities of **34a** and **34b** were also inferior to that of **25e** but were superior to those of **30a**−**c**, **31a**−**c** (Table 5). Finally, another set of experiments in a MDA-MB-231 xenograft model was conducted to compare the in vivo antitumor efficacy of **25e**, **34a**, and **34b**, with SAHA as the

dx.doi.org/10.1021/jm101605z |J. Med. Chem. 2011, 54, 2823–2838

Scheme 3. Synthesis of Compounds 30a−c and 31a−c[a]

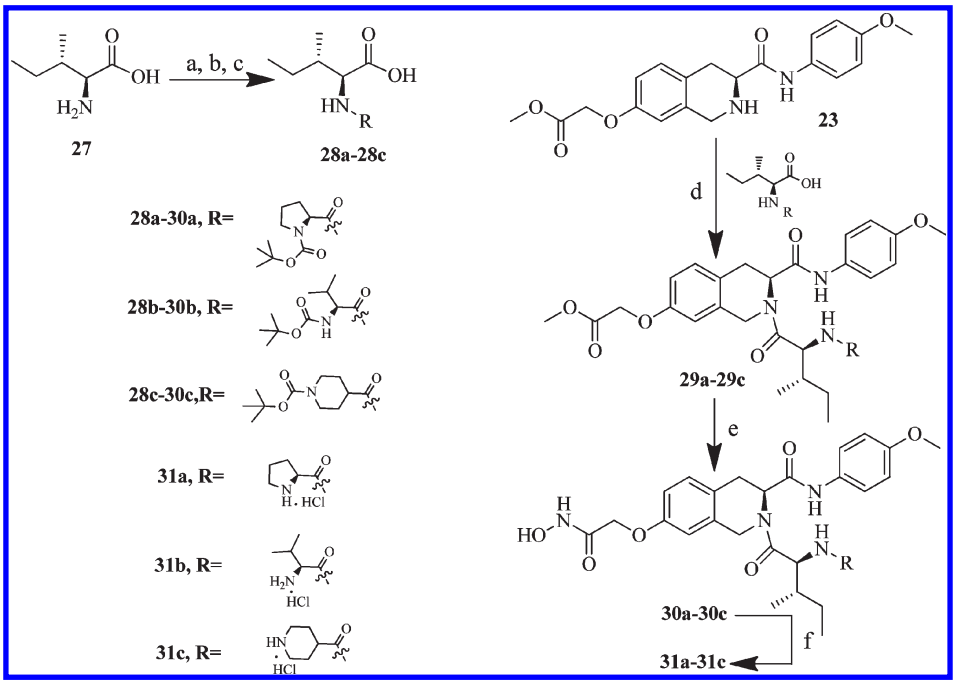

[a] Reagents and conditions: (a) HCl, CH_3OH, 96%; (b) Boc-protected amino acids, isobutyl chloroformate, NMM, THF, 74−84%; (c) 2 M NaOH, C_2H_5OH, 86-91%; (d) TBTU, Et_3N, THF, 61−67%; (e) NH_2OK, CH_3OH, 52−57%; (f) HCl, anhydrous EtOAc, 88−93%.

Scheme 4. Synthesis of Target Compounds 34a and 34b[a]

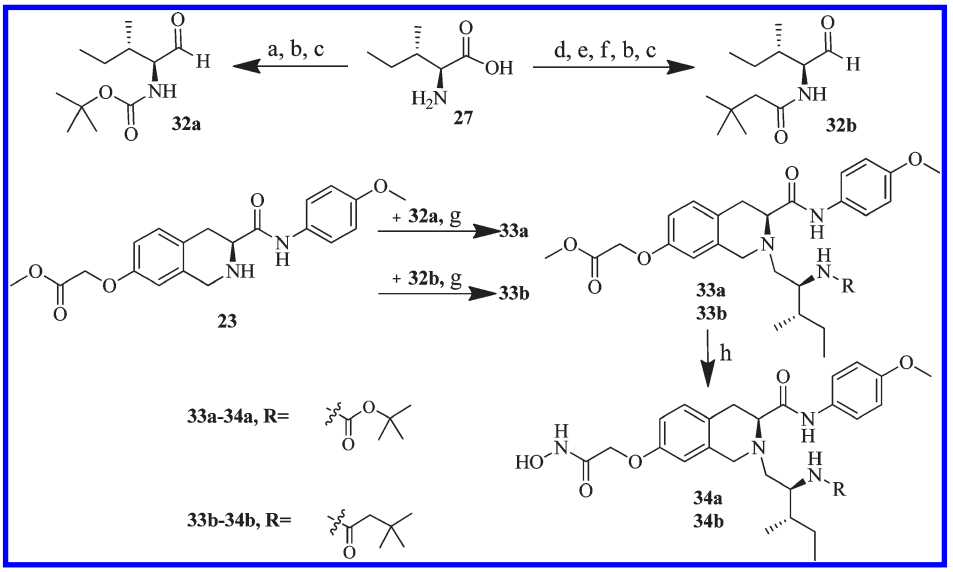

[a] Reagents and conditions: (a) $(Boc)_2O$, 1 M NaOH, THF, 89%; (b) *N,O*-dimethylhydroxylamine hydrochloride, TBTU, Et_3N, THF, 85%; (c) $LiAlH_4$, THF, 81%; (d) HCl, CH_3OH, 96%; (e) 3,3-dimethylbutyric acid, isobutyl chloroformate, NMM, THF, 87%; (f) 2 M NaOH, C_2H_5OH, 80%; (g) $(CH_3COO)_3BHNa$, 1,2-dichloroethane, 81−85%; (h) NH_2OK, CH_3OH, 55−58%.

positive control. Figure 4 shows the results in which significant tumor growth delays were observed relative to the untreated group for all of our compounds. With the exception of **34b**, all compound-treated groups were significantly different from the control group as shown by Student's two-tailed *t* test. Among these analogues, **34a** was the most effective, with a T/C value of 47% ($p < 0.01$). Meanwhile **25e** (T/C = 67%, $p < 0.05$) exhibited potency similar to that of SAHA (T/C = 70%, $p < 0.05$), which agreed well with our preceding in vivo results. The poor in vivo efficacy of **34b** (T/C = 87%, $p > 0.05$) was unexpected. We postulated that **34b** dosed as the hydrochloride might have decreased intraperitoneal absorption. However, detailed research is warranted to confirm our interpretation.

The in vitro antiproliferative activity against several solid tumor cell lines (A549, HeLa, ES-2, and MDA-MB-231) and in vivo anticancer activity in a MDA-MB-231 xenograft model

dx.doi.org/10.1021/jm101605z |*J. Med. Chem.* 2011, 54, 2823–2838

Table 1. HDAC Inhibition Activity of Compounds 7d, 22a−c, and SAHA

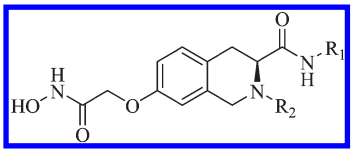

Compd	R_1	R_2	IC_{50} of HDAC8 (μM) [b]
7d[a]	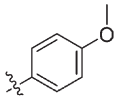	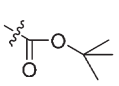	1.00±0.16
22a	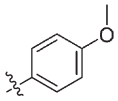	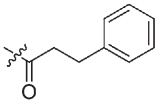	0.502±0.17
22b	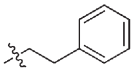	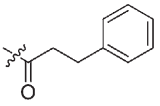	0.692±0.15
22c		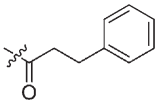	0.759±0.12
SAHA[a]			1.48±0.20

[a] Cited from ref 24. [b] Results expressed as the mean ± standard deviation of at least three separate determinations.

indicate that this series of derivatives are not HDAC8-selective inhibitors, because HDAC8 selective inhibitors, such as PCI-34051, scarcely affect the growth and viability of solid tumor cells.[29] In order to explore the HDAC isoform selectivity profile of the tetrahydroisoquinoline-based hydroxamic acid derivatives, selected compounds **25e**, **30a−c**, **31a−c**, **34a**, and **34b** were progressed to enzyme inhibition assays against HeLa cell nuclear extract (which contains primarily HDAC1 and HDAC2) and HDAC6 (representative class II HDACs). The results presented in Table 6 indicate that our tetrahydroisoquinoline-based hydroxamic acid scaffold exhibited little selectivity against individual HDACs.

Preliminary investigation of the antiproliferative mechanism was performed by treating MDA-MB-231 cells with **25e** and **34a** at different concentrations for 48 h, using SAHA as the positive control. Cell distribution by flow cytometric analysis revealed that compounds **25e** and **34a** mainly induced G1 phase arrest at low concentrations (0.5 μM); meanwhile, at increased concentrations (2 μM and 5 μM), more cells were accumulated at G2 phase (data not shown). Our results indicate that the action model of **25e** and **34a** on MDA-MB-231 cell cycle arrest is similar to that of SAHA.

Molecule Docking and Discussion. The SAR information summarized from the present research was consistent with our previously reported results. For the R_1 group in the general structure of these analogues (Figure 2), the 4-methoxyphenyl group was optimum, which could form a π−π interaction with the tyrosine 100 residue in the rim of the HDAC8 active site (Figure 5). For the R_2 group, modification and optimization could dramatically influence the hydrophobicity and steric conformation and thus the inhibitory potency for HDAC8. Generally, the more hydrophobic the R_2 group, the more potent the compound. This is supported by the fact that the hydrochloride salts (compounds **26a−h**, **31c**) were all less potent than their corresponding Boc-protected analogues (compounds **25a−h**, **30c**), because removal of the Boc group greatly decreased the hydropobicity. Besides, the result that tertiary amine analogues (**25l**, **25m**, and **25n**) were not as potent as their parent compounds (**22a**, **25i**, and **25j**) against HDAC8 also supports the importance of hydrophobicity to some extent. However, the hydrochloride salts **31a** and **31b**, which were the most potent compounds against HDAC8 in this series, seemed to be inconsistent with the aforementioned analysis. To rationalize these exceptions, possible binding modes of **31a**, **31b**, and **31c** were compared with their Boc-protected analogues **30a**, **30b**, and **30c** by docking studies (Figure 6). Compared with **30a** (Figure 6a), compound **31a** (Figure 6d) could form two more hydrogen bonds with carbonyl oxygen atom of proline 273 through amide N−H and deprotected free N−H atoms. Further, relative to **30b** (Figure 6b), compound **31b** (Figure 6e) could form three additional strong hydrogen bonds with carbonyl oxygen atoms of proline 273 and methionine 274 through amide N−H and deprotected free N−H atoms. We postulated that the additional hydrogen bonds might be the key factors that made **31a** and **31b** more effective against HDAC8 compared to their corresponding parent compounds **30a** and **30b**. However, **31c** (Figure 6f) could not form more hydrogen bonds relative to **30c** (Figure 6c). Moreover, different from **30a**, **30b**, **30c**, **31a**, and **31b**, compound **31c** could not form a π−π interaction with HDAC8 because the 4-methoxyphenyl group of **31c** was perpendicular to the tyrosine 100 residue. Therefore, the IC_{50} value of **31c** (1.44 ± 0.39 μM) was 10-fold larger than that of **30c** (0.147 ± 0.03 μM) and almost 2 orders of magnitude larger than that of **31a** (0.047 ± 0.01 μM) and **31b** (0.068 ± 0.02 μM). Although the antiproliferative activities of **31a** and **31b** were not as good as their enzyme inhibitory activities, probably because of poor cellular uptake, these two compounds could be used to probe the biological function of HDACs.

Figure 7 reveals that the low energy conformations of compounds **25e**, **34a**, and **34b**, which were optimized by the Sybyl/Sketch module, were almost the same because of their structural similarity, but as shown in Figure 8, the binding mode of compound **34b** was quite different from its analogues **25e** and **34a**. In detail, the simulative pharmacophoric conformations of **25e** and **34a** were both similar to their calculated low energy conformations, especially **34a**, which was almost accordant to its low energy conformation. However, the simulative pharmacophoric conformation of **34b** was quite different from its calculated low energy conformation. This might be the reason why compound **34a** exhibited the most potent in vivo anticancer activity but compound **34b** was essentially ineffective in the xenograft model. The real binding modes of our compounds with HDAC8 should be confirmed by further X-ray cocrystal studies. Moreover, the in vivo anticancer activities of these analogues must be closely related to their pharmacokinetic profiles. At present, related research is in progress in our lab.

Table 2. HDAC Inhibition Activity of Compounds 25a−25n, 26a−26h

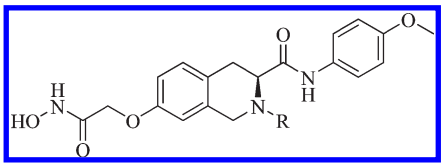

Compd	R	IC_{50} of HDAC8 (μM) [a]	Compd	R	IC_{50} of HDAC8 (μM) [a]
25a	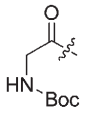	0.514±0.09	**26a**	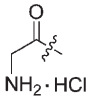	2.14±0.49
25b	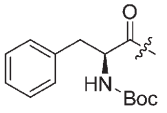	0.103±0.028	**26b**	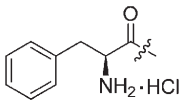	0.368±0.022
25c	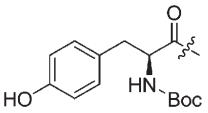	0.175±0.030	**26c**	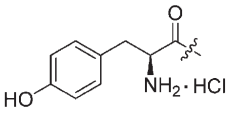	0.634±0.053
25d	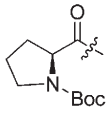	0.212±0.030	**26d**	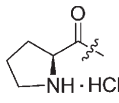	0.481±0.051
25e	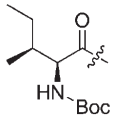	0.139±0.011	**26e**	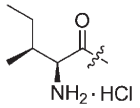	1.04±0.23
25f	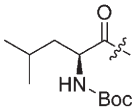	0.163±0.036	**26f**	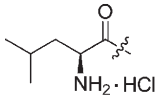	0.675±0.047
25g	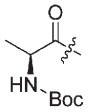	0.182±0.029	**26g**	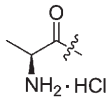	1.28±0.23
25h	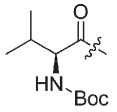	0.104±0.014	**26h**	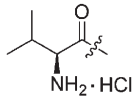	1.02±0.16
25i	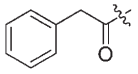	0.141±0.020	**25m**	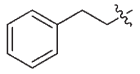	1.02±0.23
25j	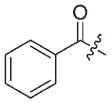	0.164±0.028	**25n**	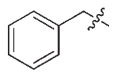	1.92±0.35
25k	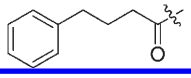	0.114±0.018	**25l**	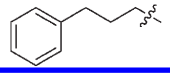	1.72±0.36

[a] Results expressed as the mean ± standard deviation of at least three separate determinations.

dx.doi.org/10.1021/jm101605z |J. Med. Chem. 2011, 54, 2823–2838

Table 3. Antiproliferative Activities of Representative Compounds against A549 and MDA-MB-231 Cell Lines

	IC_{50} (μM)[a]	
compd	A549	MDA-MB-231
22a	4.80	1.52
25b	12.7	1.29
25e	0.94	0.79
25h	0.84	1.58
25i	117	4.45
25j	5.95	3.05
25k	3.58	2.77
SAHA	0.74	1.31

[a] Values are the mean of three experiments. The standard derivations are <20% of the mean.

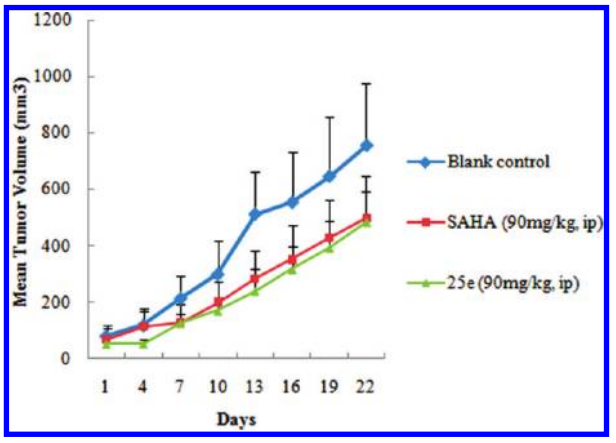

Figure 3. Antitumor activity of **25e** and SAHA against MDA-MB-231 human tumor xenografts implanted in mice, expressed as mean tumor volume.

Table 4. HDAC Inhibition Activity of 25e and Its Derivatives 30a−c, 31a−c, 34a, and 34b

compd	IC_{50} of HDAC8 (μM)[a]	compd	IC_{50} of HDAC8 (μM)[a]
30a	0.192 ± 0.04	**31a**	0.047 ± 0.01
30b	0.201 ± 0.06	**31b**	0.068 ± 0.02
30c	0.147 ± 0.03	**31c**	1.44 ± 0.39
34a	0.263 ± 0.04	**34b**	0.333 ± 0.04
25e	0.139 ± 0.011		

[a] Results expressed as the mean ± standard deviation of at least three separate determinations.

CONCLUSION

A series of tetrahydroisoquinoline-based hydroxamic acids have been described as HDAC inhibitors in our previous work. In our present research, further derivatization that focused on the most potent compound **7d** led to another novel series of compounds exhibiting low micromolar to mid-nanomolar IC_{50} values in the in vitro HDAC inhibition assay and antiproliferative assay. Several compounds, **25e**, **34a**, and **34b**, were evaluated for their in vivo antitumor study in a MDA-MB-231 xenograft mice model and showed efficacy comparable to the that of approved drug SAHA. More detailed studies of the antitumor profiles of these promising compounds are underway in our lab. Using **25e**, **34a**, and **34b** as leads, continued efforts are underway to search more potent HDACi.

Table 5. Antiproliferative Activities of Representative Compounds against Several Tumor Cell Lines

	IC_{50} (μM)[a]					
compd	HeLa	K562	NB4	HL60	ES-2	MDA-MB-231
25e	37.1	1.47	1.50	47.6	5.0	0.79
30a	184	2.32	5.15	76.8	ND	ND[b]
30b	167	2.78	63.3	ND	ND	ND
30c	>200	12.3	68.2	ND	ND	ND
31a	>200	6.59	9.28	69.8	ND	ND
31b	118	20.4	69.9	ND	ND	ND
31c	102	51.7	>200	ND	ND	ND
34a	29.2	7.0	3.87	42.7	7.20	2.20
34b	63.5	10.0	5.57	25.7	ND	2.54
SAHA	147	3.32	1.52	>200	6.21	1.31

[a] Values are the mean of three experiments. The standard derivations are <20% of the mean. [b] Not determined.

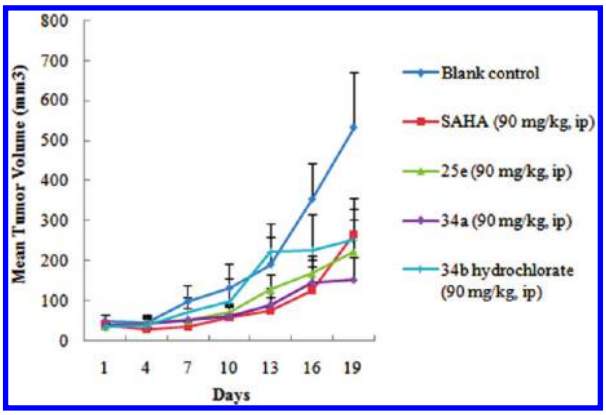

Figure 4. Antitumor activity comparison of **25e**, **34a**, **34b**, and SAHA against MDA-MB-231 human tumor xenografts implanted in mice, expressed as mean tumor volume.

EXPERIMENT SECTION

Materials and Methods. All commercially available starting materials, reagents, and solvents were used without further purification unless otherwise stated. All reactions were monitored by TLC with 0.25 mm silica gel plates (60GF-254). UV light, iodine stain, and ferric chloride were used to visualize the spots. Silica gel or C18 silica gel was used for column chromatography purification. Microwave-aided synthesis was performed using a CEM Discover-S microwave synthesis system. ^{1}H NMR spectra were recorded on a Bruker DRX spectrometer at 600 MHz, δ in parts per million and J in hertz, using TMS as an internal standard. High-resolution mass spectra were conducted by Shandong Analysis and Test Center in Ji'nan, China. ESI-MS spectra were recorded on an API 4000 spectrometer. Melting points were determined uncorrected on an electrothermal melting point apparatus. All tested compounds are >95% pure by HPLC analysis, performed on a Agilent 1100 HPLC instrument using a Phenomenex Synergi 4 μ Hydro-RP 80A column (250 mm ×4.6 mm) according to one of the

dx.doi.org/10.1021/jm101605z |J. Med. Chem. 2011, 54, 2823–2838

Table 6. HDAC Inhibition Activity and Isoform Selectivity of 25e, 30a−c, 31a−31c, 34a, and 34b

compd	IC_{50} of HeLa nuclear extract (μM)[a]	IC_{50} of HDAC6 (μM)[a]	IC_{50} of HDAC8 (μM)	HDAC8/HeLa nuclear extract isoform selectivity	HDAC8/HDAC6 isoform selectivity
25e	0.058	0.047	0.139	2.40	2.96
30a	0.065	0.141	0.192	2.95	1.36
30b	0.128	0.116	0.201	1.57	1.73
30c	0.214	0.164	0.147	0.69	0.90
31a	0.108	0.191	0.047	0.44	0.25
31b	0.073	0.163	0.068	0.93	0.42
31c	0.071	0.169	1.44	2.03	0.85
34a	0.447	0.094	0.263	0.59	2.80
34b	0.297	0.158	0.333	1.12	2.11
SAHA	0.107	0.195	1.48	13.8	7.60

[a] Values are the mean of at least two separate determinations.

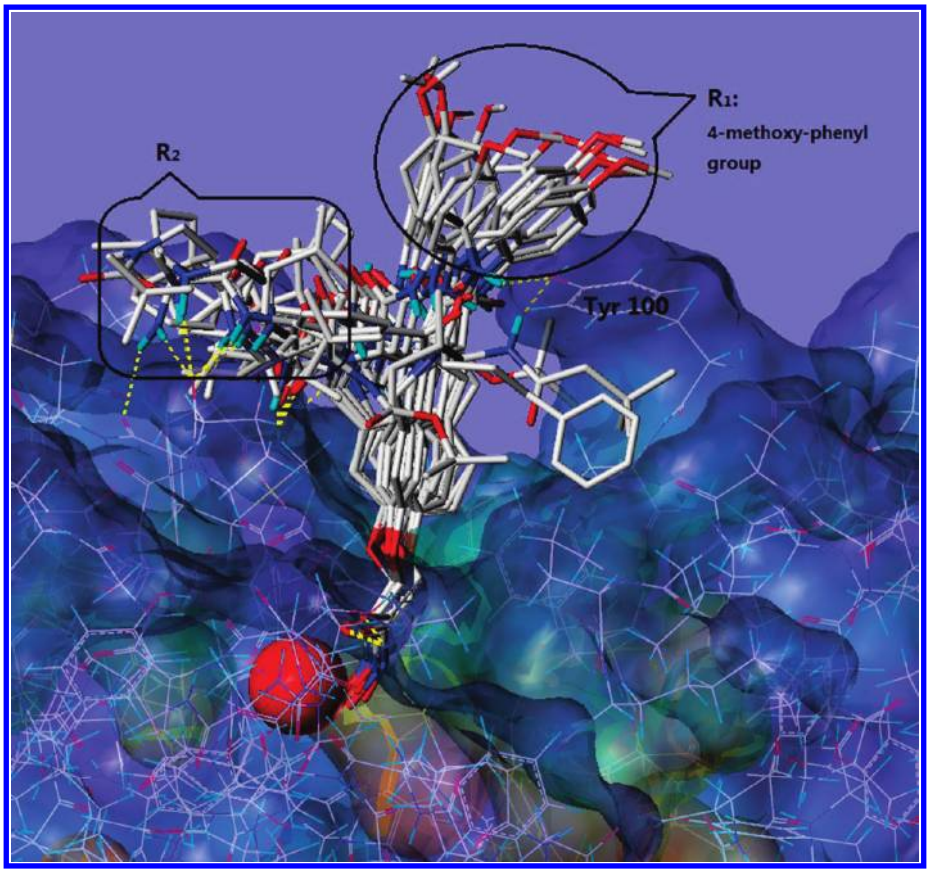

Figure 5. Superposition of several tetrahydroisoquinoline-derived HDACi with potent HDAC8 inhibitory activity (compounds **22a**, **25b**, **25e**, **25h**, **25i**, **25j**, **25k**, **30a**, **30b**, **30c**, **31a**, **31b**, **31c**, **34a**, **34b**) revealed their proposed binding modes at the HDAC8 active site. The zinc ion is shown as a red sphere.

following methods. Method A: compounds **22a−c**, **25a−n**, **30a−c**, **34a**, and **34b** were eluted with 50% acetonitrile/50% water (containing 0.1% formic acid) over 20 min, with detection at 254 nm and a flow rate of 1.8 mL/min. Method B: compounds **26a−h** and **31a−c** were eluted with 25% acetonitrile/75% water (containing 0.1% formic acid) over 20 min, with detection at 254 nm and a flow rate of 1.5 mL/min.

(*S*)-7-Hydroxy-6,8-diiodo-Tic hydrochloride (**16**), (*S*)-2-(*tert*-Butoxycarbonyl)-7- hydroxy-6,8-diiodo-Tic (**17**), (*S*)-2-(*tert*-Butoxycarbonyl)-7-hydroxy-Tic (**18**), (*S*)-*tert*-Butyl 7-Hydroxy-3-((4-methoxyphenyl)carbamoyl)-3,4-dihydroisoquinoline -2(1H)-carboxylate (**19a**) and its analogues (**19b**, **19c**), and (*S*)-*tert*-Butyl 7-(2-Methoxy-2-oxoethoxy)-3-((4-methoxyphenyl)carbamoyl)-3,4-dihydroisoquinoline-2(1*H*)-carboxylate (**20a**) and its analogues (**20b**, **20c**) were synthesized as described previously.[24] Dipeptides **28a−c** were synthesized according to the procedures described previously.[31] Aldehydes **32a** and **32b** were obtained from their corresponding carboxylic acid compounds according to a similar literature method.[25]

General Procedure for the Preparation of 21a and Its Analogues 21b, 21c, 24a−k, 29a−c. (*S*)-Methyl 2-(3-(4-Methoxyphenylcarbamoyl)-2-(3-phenylpropanoyl)-1,2,3,4-tetrahydroisoquinolin-7-yloxy)acetate (21a). To a solution of **20a** (4.71 g, 10.0 mmol) in anhydrous dichloromethane (40 mL) was

dx.doi.org/10.1021/jm101605z |*J. Med. Chem.* 2011, 54, 2823–2838

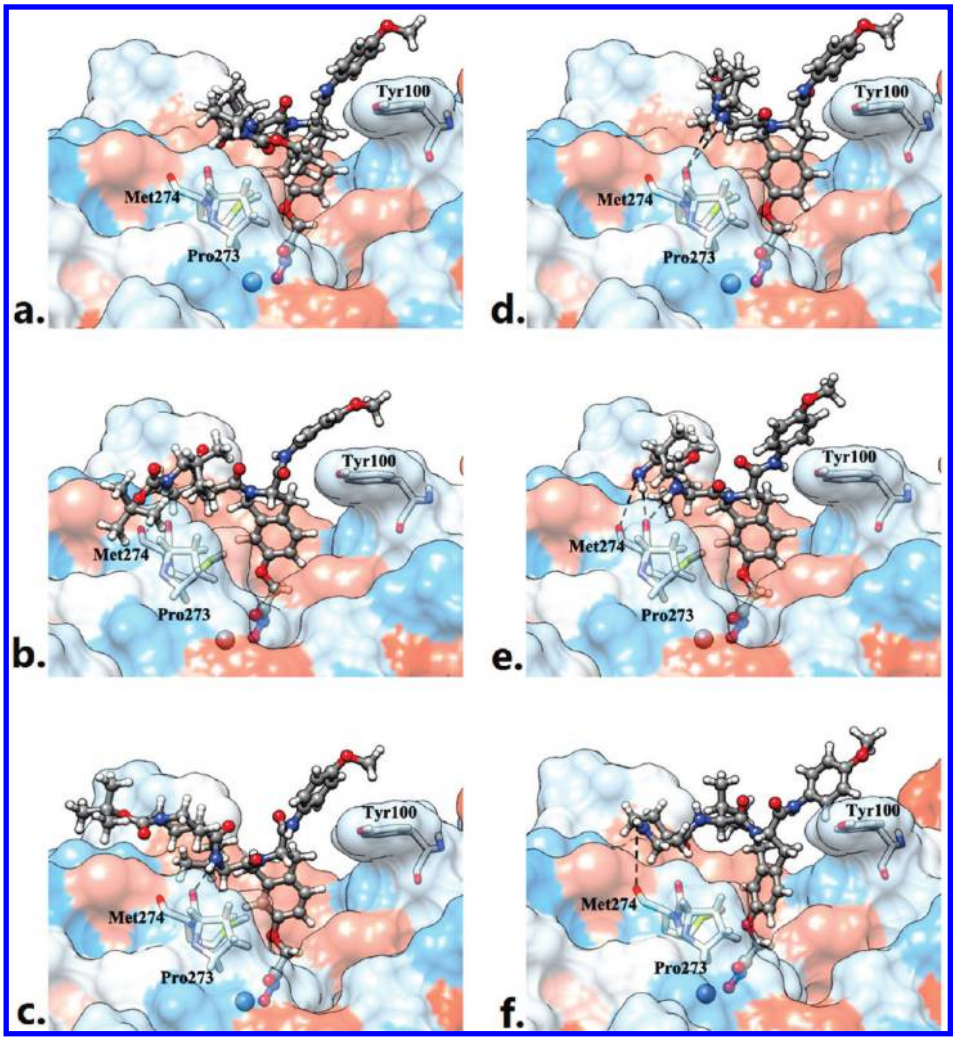

Figure 6. Proposed binding preferences comparison of compounds **30a** (a), **30b** (b), **30c** (c), **31a** (d), **31b** (e), and **31c** (f) at HDAC8. Protein is represented by the molecular surface, and the amino acid residues are represented in stick mode. The dashed lines stand for the hydrogen bonds. The pictures were produced using UCSF chimera software[30] (atom types: H, white; N, blue; O, red; S, yellow).

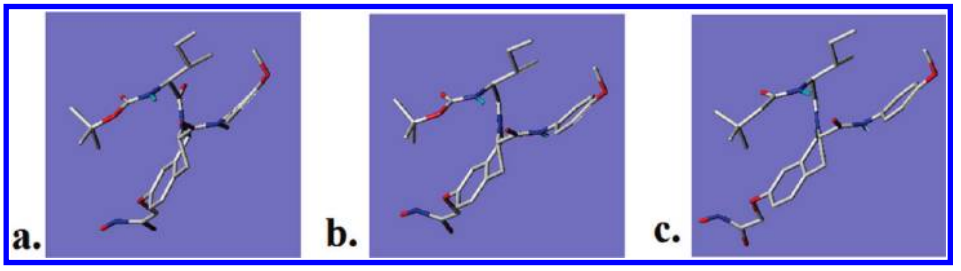

Figure 7. Calculated low energy conformations of **25e** (a), **34a** (b), and **34b** (c).

added trifluoroacetic acid (15 mL). When the reaction was finished, saturated Na_2CO_3 was added to the solution until the pH became weakly basic. The mixture was separated with a separatory funnel, and the organic layer was washed with distilled water, dried over $MgSO_4$, and evaporated under vacuum to obtain 3.45 g of secondary amine **23** as a white solid. This product was used for the subsequent reaction without further purification. ^{1}H NMR (DMSO-d_6) δ 2.72 (s, 1H), 2.74 (dd, J = 10.2 Hz, J = 15.6 Hz, 1H), 2.91 (dd, J = 4.8 Hz, J = 15.6 Hz, 1H), 3.54 (dd, J = 4.8 Hz, J = 10.2 Hz, 1H), 3.69 (s, 3H), 3.72 (s, 3H), 3.87−3.95 (m, 2H), 4.74 (s, 2H), 6.64 (d, J = 2.4 Hz, 1H), 6.72 (dd, J = 2.4 Hz, J = 8.4 Hz, 1H), 6.88 (d, J = 9.0 Hz, 2H), 7.05 (d, J = 8.4 Hz, 1H), 7.58 (d, J = 9.0 Hz, 2H), 9.75 (s, 1H). ESI-MS m/z: 371.3 $[M + H]^+$.

At room temperature, to a solution of 3-phenylpropionic acid (0.75 g, 5.0 mmol) in anhydrous THF (20 mL) was added Et_3N (0.56 g, 5.5 mmol) followed by 2-(1*H*-benzotriazol-1-yl)-1,1,3,3-tetramethyluronium tetrafluoroborate (TBTU, 1.78 g, 5.5 mmol). After 15 min, the amine compound **23** (1.85 g, 5.0 mmol) was added. Stirring was continued for 8 h, and then THF was evaporated with the residue being taken up in EtOAc

dx.doi.org/10.1021/jm101605z |*J. Med. Chem.* 2011, 54, 2823–2838

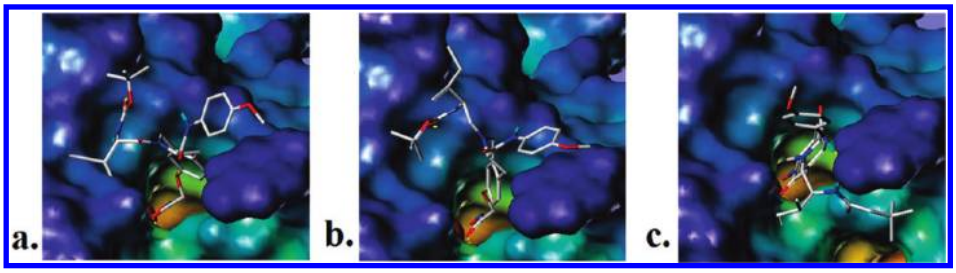

Figure 8. Proposed binding mode comparison of compounds **25e** (a), **34a** (b), and **34b** (c) at HDAC8. Protein is represented by the molecular surface, and the zinc ion is shown in red (atom types: polar H, sky-blue; N, dark blue; O, red).

(40 mL). The EtOAc solution was washed with saturated Na_2CO_3 (3 × 10 mL) and brine (3 × 10 mL), dried over $MgSO_4$, and evaporated under vacuum. The crude product was purified by flash column chromatography (petroleum ether/EtOAc 2:1) to give desired compound **21a** (1.53 g, 61% yield) as a colorless oil, which crystallized upon standing. ^{1}H NMR (DMSO-d_6) δ 2.78−2.87 (m, 4H), 3.02−3.16 (m, 2H), 3.68 (s, 3H), 3.70 (s, 3H), 4.66 (d, J = 15.6 Hz, 1H), 4.72 (d, J = 15.6 Hz, 1H), 4.74 (s, 2H), 5.01−5.04 (m, 1H), 6.77−6.88 (m, 2H), 7.09−7.12 (m, 1H), 7.15−7.29 (m, 7H), 7.35−7.39 (m, 2H), 9.74 (s, 1H). ESI-MS m/z: 503.2 $[M + H]^+$.

(*S*)-Methyl 2-(3-(Phenethylcarbamoyl)-2-(3-phenylpropanoyl)-1,2,3,4-tetrahydroisoquinolin-7-yloxy)acetate (21b). Colorless oil crystallized upon standing, 67% yield. ^{1}H NMR (DMSO-d_6) δ 2.48−2.85 (m, 8H), 2.95−3.08 (m, 2H), 3.68 (s, 3H), 4.44−4.65 (m, 2H), 4.72 (s, 2H), 4.98−5.00 (m, 1H), 6.75−6.80 (m, 3H), 7.04−7.08 (m, 2H), 7.16−7.31 (m, 8H), 7.98 (s, 1H). ESI-MS m/z: 501.3 $[M + H]^+$.

(*S*)-Methyl 2-(3-(Phenylcarbamoyl)-2-(3-phenylpropanoyl)-1,2,3,4-tetrahydroisoquinolin-7-yloxy)acetate (21c). Colorless oil crystallized upon standing, 60% yield. ^{1}H NMR (DMSO-d_6) δ 2.81−2.88 (m, 4H), 3.07−3.15 (m, 2H), 3.67 (s, 3H), 4.63 (d, J = 15.6 Hz, 1H), 4.69 (d, J = 15.6 Hz, 1H), 4.71 (s, 2H), 5.02−5.04 (m, 1H), 6.77−6.86 (m, 2H), 7.01−7.03 (m, 1H), 7.11−7.31 (m, 8H), 7.45−7.52 (m, 2H), 9.99 (s, 1H). ESI-MS m/z: 473.2 $[M + H]^+$.

(*S*)-Methyl 2-(2-(2-(*tert*-Butoxycarbonylamino)acetyl)-3-(4-methoxyphenylcarbamoyl)-1,2,3,4-tetrahydroisoquinolin-7-yloxy)acetate (24a). Colorless oil crystallized upon standing, 67% yield. ^{1}H NMR (DMSO-d_6) δ 1.30 + 1.36 (s, 9H, cis/trans), 3.07−3.19 (m, 2H), 3.68 (s, 3H), 3.70 (s, 3H), 3.93−4.04 (m, 2H), 4.62 (d, J = 15.6 Hz, 1H), 4.71 (d, J = 15.6 Hz, 1H), 4.72 (s, 2H), 4.93−4.95 (m, 1H), 6.77−6.86 (m, 5H), 7.12−7.14 (m, 1H), 7.36−7.40 (m, 2H), 9.88 (s, 1H). ESI-MS m/z: 528.2 $[M + H]^+$.

Methyl 2-((*S*)-2-((*S*)-2-(*tert*-Butoxycarbonylamino)-3-phenylpropanoyl)-3-(4-methoxyphenylcarbamoyl)-1,2,3,4-tetrahydroisoquinolin-7-yloxy)acetate (24b). Colorless oil crystallized upon standing, 60% yield. ^{1}H NMR (DMSO-d_6) δ 1.27 + 1.20 (s, 9H, cis/trans), 2.80−2.91 (m, 2H), 3.00−3.15 (m, 2H), 3.68 (s, 3H), 3.70 (s, 3H), 4.65 (d, J = 15.6 Hz, 1H), 4.76 (d, J = 15.6 Hz, 1H), 4.70 (s, 2H), 4.80−5.01 (m, 2H), 6.70−6.96 (m, 4H), 7.05−7.30 (m, 5H), 7.37−7.49 (m, 4H), 9.85 (s, 1H). ESI-MS m/z: 618.3 $[M + H]^+$.

Methyl 2-((*S*)-2-((*S*)-2-(*tert*-Butoxycarbonylamino)-3-(4-hydroxyphenyl)propanoyl)-3-(4-methoxyphenylcarbamoyl)-1,2,3,4-tetrahydroisoquinolin-7-yloxy)acetate (24c). Colorless oil crystallized upon standing, 64% yield.

(*S*)-*tert*-Butyl 2-((*S*)-7-(2-Methoxy-2-oxoethoxy)-3-(4-methoxyphenylcarbamoyl)-1,2,3,4-tetrahydroisoquinoline-2-carbonyl)pyrrolidine-1-carboxylate (24d). Colorless oil crystallized upon standing, 61% yield.

Methyl 2-((*S*)-2-((2*S*,3*S*)-2-(*tert*-Butoxycarbonylamino)-3-methylpentanoyl)-3-(4-methoxyphenylcarbamoyl)-1,2,3,4-tetrahydroisoquinolin-7-yloxy)acetate (24e). Colorless oil crystallized upon standing, 59% yield.

Methyl 2-((*S*)-2-((*S*)-2-(*tert*-Butoxycarbonylamino)-4-methylpentanoyl)-3-(4-methoxyphenylcarbamoyl)-1,2,3,4-tetrahydroisoquinolin-7-yloxy)acetate (24f). Colorless oil crystallized upon standing, 63% yield.

Methyl 2-((*S*)-2-((*S*)-2-(*tert*-Butoxycarbonylamino)propanoyl)-3-(4-methoxyphenylcarbamoyl)-1,2,3,4-tetrahydroisoquinolin-7-yloxy)acetate (24g). Colorless oil crystallized upon standing, 67% yield.

Methyl 2-((*S*)-2-((*S*)-2-(*tert*-Butoxycarbonylamino)-3-methylbutanoyl)-3-(4-methoxyphenylcarbamoyl)-1,2,3,4-tetrahydroisoquinolin-7-yloxy)acetate (24h). Colorless oil crystallized upon standing, 66% yield.

(*S*)-Methyl 2-(3-(4-Methoxyphenylcarbamoyl)-2-(2-phenylacetyl)-1,2,3,4-tetrahydroisoquinolin-7-yloxy)acetate (24i). Colorless oil crystallized upon standing, 61% yield.

(*S*)-Methyl 2-(2-Benzoyl-3-(4-methoxyphenylcarbamoyl)-1,2,3,4-tetrahydroisoquinolin-7-yloxy)acetate (24j). Colorless oil crystallized upon standing, 67% yield.

(*S*)-Methyl 2-(3-(4-Methoxyphenylcarbamoyl)-2-(4-phenylbutanoyl)-1,2,3,4-tetrahydroisoquinolin-7-yloxy)acetate (24k). Colorless oil crystallized upon standing, 66% yield.

(*S*)-*tert*-Butyl 2-((2*S*,3*S*)-1-((*S*)-7-(2-Methoxy-2-oxoethoxy)-3-(4-methoxyphenylcarbamoyl)-3,4-dihydroisoquinolin-2(1*H*)-yl)-3-methyl-1-oxopentan-2-ylcarbamoyl)pyrrolidine-1-carboxylate (29a). Colorless oil crystallized upon standing, 64% yield. ^{1}H NMR (DMSO-d_6) δ 0.71−0.93 (m, 6H), 1.03−1.43 (m, 11H), 1.54−1.87 (m, 4H), 2.05−2.13 (m, 1H), 2.98−3.36 (m, 4H), 3.69 (s, 3H), 3.70 (s, 3H), 4.16−4.29 (m, 1H), 4.54−4.72 (m, 1H), 4.70 (s, 2H), 4.74−4.86 (m, 2H), 4.90−5.15 (m, 1H), 6.72−6.86 (m, 4H), 7.02−7.13 (m, 1H), 7.35−7.53 (m, 2H), 7.95−8.44 (m, 1H), 9.43−10.07 (m, 1H). ESI-MS m/z: 681.4 $[M + H]^+$.

Methyl 2-((*S*)-2-((2*S*,3*S*)-2-((*S*)-2-(*tert*-Butoxycarbonylamino)-3-methylbutanamido)-3-methylpentanoyl)-3-(4-methoxyphenylcarbamoyl)-1,2,3,4-tetrahydroisoquinolin-7-yloxy)acetate (29b). Colorless oil crystallized upon standing, 61% yield. ^{1}H NMR (DMSO-d_6) δ 0.71−0.96 (m, 12H), 1.10−1.19 (m, 1H), 1.20−1.29 (m, 1H), 1.32 + 1.37 (s, 9H, cis/trans), 1.68−1.78 (m, 1H), 1.81−2.00 (m, 1H), 2.98−3.25 (m, 2H), 3.68 (s, 3H), 3.69 (s, 3H), 3.75−3.95 (m, 1H), 4.50−5.13 (m, 4H), 4.71 (s, 2H), 6.60−6.90 (m, 4H), 7.05−7.12 (m, 1H), 7.33−7.52 (m, 2H), 7.88 (s, 1H), 8.09 (s, 1H), 9.87 (s, 1H). ESI-MS m/z: 683.4 $[M + H]^+$.

***tert*-Butyl 4-((2*S*,3*S*)-1-((*S*)-7-(2-Methoxy-2-oxoethoxy)-3-(4-methoxyphenylcarbamoyl)-3,4-dihydroisoquinolin-2(1*H*)-yl)-3-methyl-1-oxopentan-2-ylcarbamoyl)piperidine-1-carboxylate (29c).** Colorless oil crystallized upon standing, 67% yield. ^{1}H NMR (DMSO-d_6) δ 0.80−0.96 (m, 6H), 1.09−1.17 (m, 1H), 1.31−1.37 (m, 1H), 1.39 (s, 9H), 1.46−1.58 (m, 2H), 1.66−1.70 (m, 2H), 1.72−1.81 (m, 1H), 2.38−2.57 (m, 1H), 2.58−2.77 (m, 2H), 2.96−3.25 (m, 2H), 3.67 (s, 3H), 3.69 (s, 3H), 3.85−4.01 (m, 2H), 4.51−5.09 (m, 4H), 4.72 (s, 2H), 6.72−6.93 (m, 4H), 7.07−7.16 (m, 1H), 7.33−7.51 (m, 2H), 8.23 (s, 1H), 9.86 (s, 1H). ESI-MS m/z: 695.4 $[M + H]^+$.

General Procedure for the Preparation of 24l and Its Analogue 24m. (*S*)-Methyl 2-(3-(4-Methoxyphenylcarbamoyl)-2-(3-phenylpropyl)-1,2,3,4-tetrahydroisoquinolin-7-yloxy)acetate (24l). A sealed tube containing compound **23** (0.15 g, 0.41 mmol), potassium carbonate powder (0.084 g, 0.61 mmol), (3-bromopropyl)benzene (0.12 g, 0.61 mmol), and DMF (4 mL) was subjected to microwave irradiation at 70 °C for 20 min, at 100 W. After cooling, the mixture was poured into 20 mL of water and extracted with EtOAc (3 × 10 mL). The organic layers were combined, washed with brine (3 × 10 mL), dried over $MgSO_4$, and evaporated under vacuum. The residue was purified by flash column chromatography (petroleum ether/EtOAc 3:1) to give desired compound **24l** (0.16 g, 81% yield) as colorless oil. ^{1}H NMR (DMSO-d_6) δ 1.82−1.85 (m, 2H), 2.58−2.60 (m, 4H), 2.91−2.94 (m, 2H), 3.51−3.52 (m, 1H), 3.67 (s, 3H), 3.69 (d, J = 15.6 Hz, 1H), 3.71 (s, 3H), 4.03 (d, J = 15.6 Hz, 1H), 4.73 (s, 2H), 6.72−6.74 (m, 2H), 6.86 (d, J = 9.0 Hz, 2H), 7.05−7.06 (m, 1H), 7.12−7.24 (m, 5H), 7.51 (d, J = 9.0 Hz, 2H), 9.74 (s, 1H).

(*S*)-Methyl 2-(3-(4-Methoxyphenylcarbamoyl)-2-phenethyl-1,2,3,4-tetrahydroisoquinolin-7-yloxy)acetate (24m). Colorless oil, 75% yield.

(*S*)-Methyl 2-(2-Benzyl-3-(4-methoxyphenylcarbamoyl)-1,2,3,4-tetrahydroisoquinolin-7-yloxy)acetate (24n). A mixture of **23** (0.4 g, 1.08 mmol), potassium carbonate powder (0.22 g, 1.62 mmol), and benzyl bromide (0.28 g, 1.62 mmol) in anhydrous DMF (15 mL) was stirred at room temperature for 4 h. The mixture was poured into 60 mL of water and extracted with EtOAc (3 × 20 mL). The organic layers were combined, washed with brine (3 × 15 mL), dried over $MgSO_4$, and evaporated under vacuum. The residue was purified by flash column chromatography (petroleum ether/EtOAc 3:1) to give desired compound **24n** (0.43 g, 86% yield) as colorless oil. ^{1}H NMR (DMSO-d_6) δ 2.97−3.06 (m, 2H), 3.60−3.65 (m, 3H), 3.67 (s, 3H), 3.71 (s, 3H), 3.76−3.89 (m, 2H), 4.75 (s, 2H), 6.61 (d, J = 2.4 Hz, 1H), 6.72 (dd, J = 2.4 Hz, J = 8.4 Hz, 1H), 6.87 (d, J = 7.2 Hz, 2H), 7.07 (d, J = 8.4 Hz, 1H), 7.26 (t, J = 7.2 Hz, 1H), 7.34 (d, J = 7.2 Hz, 2H), 7.41 (d, J = 7.2 Hz, 2H), 7.54 (d, J = 7.2 Hz, 2H), 9.86 (s, 1H).

General Procedure for the Preparation of 33a and Its Analogues 33b. Methyl 2-((*S*)-2-((2*S*,3*S*)-2-(*tert*-Butoxycarbonylamino)-3-methylpentyl)-3-(4-methoxyphenylcarbamoyl)-1,2,3,4-tetrahydroisoquinolin-7-yloxy)acetate (33a). To a solution of compound **23** (0.37 g, 1.0 mmol) and **32a** (0.24 g, 1.1 mmol) in 1,2-dichloroethane (20 mL) was added sodium triacetoxyborohydride (0.32 g, 1.5 mmol). The mixture was stirred at room temperature for 4 h, and the solvent was evaporated under vacuum. The residue was taken up by EtOAc (30 mL), washed with saturated Na_2CO_3 (3 × 10 mL) and brine (3 × 10 mL), dried over $MgSO_4$, and evaporated to get the crude product, which was purified by flash column chromatography (petroleum ether/EtOAc 3:1) to give desired compound **33a** (0.46 g, 81% yield) as colorless oil crystallized upon standing.

Methyl 2-((*S*)-2-((2*S*,3*S*)-2-(3,3-Dimethylbutanamido)-3-methylpentyl)-3-(4-methoxyphenylcarbamoyl)-1,2,3,4-tetrahydroisoquinolin-7-yloxy)acetate (33b). Colorless oil crystallized upon standing, 85% yield.

General Procedure for the Preparation of 22a and Its Analogues 22b, 22c, 25a−25n, 30a−30c, 34a, 34b. (*S*)-7-(2-(Hydroxyamino)-2-oxoethoxy)-*N*-(4-methoxyphenyl)-2-(3-phenylpropanoyl)-1,2,3,4-tetrahydroisoquinoline-3-carboxamide (22a). To a solution of compound **21a** (1.0 g, 2.0 mmol) in 10 mL of anhydrous methanol was added a solution of NH_2OK (0.14 g, 6 mmol) in 3.5 mL of anhydrous methanol. The mixture was stirred for 0.5 h, and the solvent was evaporated under vacuum. The residue was acidified with 2 N HCl until pH 5−6 and then extracted with EtOAc (3 × 10 mL). The organic layers were combined, washed with brine (3 × 10 mL), dried over $MgSO_4$, and evaporated with the residue being purified by C18 reversed-phase column chromatography (H_2O/MeOH 3:7) to give desired compound **22a** (0.59 g, 59% yield) as a white powder. Mp: 174−176 °C. ^{1}H NMR (DMSO-d_6) δ 2.79−2.87 (m, 4H), 3.03−3.18 (m, 2H), 3.70 (s, 3H), 4.42 (s, 2H), 4.65 (d, J = 15.6 Hz, 1H), 4.72 (d, J = 15.6 Hz, 1H), 5.01−5.03 (m, 1H), 6.76−6.87 (m, 2H), 7.09−7.12 (m, 1H), 7.15−7.29 (m, 7H), 7.35−7.39 (m, 2H), 8.97 (s, 1H), 9.74 (s, 1H), 10.81 (s, 1H). HRMS (AP-ESI) m/z calcd for $C_{28}H_{30}N_3O_6$ $[M + H]^+$ 504.2135, found 504.2141. Retention time: 2.6 min.

(*S*)-7-(2-(Hydroxyamino)-2-oxoethoxy)-*N*-phenethyl-2-(3-phenylpropanoyl)-1,2,3,4-tetrahydroisoquinoline-3-carboxamide (22b). White powder, 56% yield. Mp: 146−148 °C. ^{1}H NMR (DMSO-d_6) δ 2.52−2.86 (m, 8H), 3.10−3.20 (m, 2H), 4.40 (s, 2H), 4.53 (d, J = 15.6 Hz, 1H), 4.65 (d, J = 15.6 Hz, 1H), 4.98−5.00 (m, 1H), 6.76−6.80 (m, 3H), 7.03−7.06 (m, 2H), 7.14−7.30 (m, 8H), 7.90 (s, 1H), 8.96 (s, 1H), 10.81 (s, 1H). HRMS (AP-ESI) m/z calcd for $C_{29}H_{31}N_3NaO_5$ $[M + Na]^+$ 524.2161, found 524.2198. Retention time: 2.9 min.

(*S*)-7-(2-(Hydroxyamino)-2-oxoethoxy)-*N*-phenyl-2-(3-phenylpropanoyl)-1,2,3,4-tetrahydroisoquinoline-3-carboxamide (22c). White powder, 56% yield. Mp: 167−169 °C. ^{1}H NMR (DMSO-d_6) δ 2.81−2.88 (m, 4H), 3.08−3.17 (m, 2H), 4.42 (s, 2H), 4.63 (d, J = 15.6 Hz, 1H), 4.73 (d, J = 15.6 Hz, 1H), 5.02−5.04 (m, 1H), 6.76−6.88 (m, 2H), 7.01−7.03 (m, 1H), 7.10−7.30 (m, 8H), 7.46−7.50 (m, 2H), 8.96 (s, 1H), 9.99 (s, 1H), 10.81 (s, 1H). HRMS (AP-ESI) m/z calcd for $C_{27}H_{28}N_3O_5$ $[M + H]^+$ 474.2029, found 474.2036. Retention time: 2.9 min.

(*S*)-*tert*-Butyl 2-(7-(2-(Hydroxyamino)-2-oxoethoxy)-3-(4-methoxyphenylcarbamoyl)-3,4-dihydroisoquinolin-2(1*H*)-yl)-2-oxoethylcarbamate (25a). White powder, 52% yield. Mp: 178−180 °C. ^{1}H NMR (DMSO-d_6) δ 1.31 + 1.37 (s, 9H, cis/trans), 3.08−3.20 (m, 2H), 3.70 (s, 3H), 3.94−4.04 (m, 2H), 4.42 (s, 2H), 4.62 (d, J = 15.6 Hz, 1H), 4.71 (d, J = 15.6 Hz, 1H), 4.93−4.95 (m, 1H), 6.76−6.87 (m, 5H), 7.11−7.14 (m, 1H), 7.37−7.41 (m, 2H), 8.97 (s, 1H), 9.87 (s, 1H), 10.83 (s, 1H). HRMS (AP-ESI) m/z calcd for $C_{26}H_{33}N_4O_8$ $[M + H]^+$ 529.2298, found 529.2300. Retention time: 2.1 min.

***tert*-Butyl (*S*)-1-((*S*)-7-(2-(Hydroxyamino)-2-oxoethoxy)-3-(4-methoxyphenylcarbamoyl)-3,4-dihydroisoquinolin-2(1*H*)-yl)-1-oxo-3-phenylpropan-2-ylcarbamate (25b).** White powder, 55% yield. Mp: 125−127 °C. ^{1}H NMR (DMSO-d_6) δ 1.26 + 1.29 (s, 9H, cis/trans), 2.79−2.92 (m, 2H), 3.00−3.16 (m, 2H), 3.70 (s, 3H), 4.44 (s, 2H), 4.66 (d, J = 15.6 Hz, 1H), 4.78 (d, J = 15.6 Hz, 1H), 4.80−5.00 (m, 2H), 6.71−6.95 (m, 4H), 7.06−7.32 (m, 5H), 7.37−7.49 (m, 4H), 8.96 (s, 1H), 9.84 (s, 1H), 10.81 (s, 1H). HRMS (AP-ESI) m/z calcd for $C_{33}H_{38}N_4NaO_8$ $[M + Na]^+$ 641.2587, found 641.2603. Retention time: 4.9 min.

***tert*-Butyl (*S*)-1-((*S*)-7-(2-(Hydroxyamino)-2-oxoethoxy)-3-(4-methoxyphenylcarbamoyl)-3,4-dihydroisoquinolin-2(1*H*)-yl)-3-(4-hydroxyphenyl)-1-oxopropan-2-ylcarbamate (25c).** White powder, 54% yield. Mp: 152−154 °C. ^{1}H NMR (DMSO-d_6) δ 1.28 + 1.32 (s, 9H, cis/trans), 2.67−2.89 (m, 2H), 3.02−3.14 (m, 2H), 3.71 (s, 3H), 4.48 (s, 2H), 4.62−4.97 (m, 4H), 6.58−6.72 (m, 3H), 6.79−6.87 (m, 3H), 6.95−7.23 (m, 4H), 7.41−7.44 (m, 2H), 8.95 (s, 1H), 9.18 (s, 1H), 9.83 (s, 1H), 10.81 (s, 1H). HRMS (AP-ESI) m/z calcd for $C_{33}H_{38}N_4NaO_9$ $[M + Na]^+$ 657.2536, found 657.2541. Retention time: 2.7 min.

(*S*)-*tert*-Butyl 2-((*S*)-7-(2-(Hydroxyamino)-2-oxoethoxy)-3-(4-methoxyphenylcarbamoyl)-1,2,3,4-tetrahydroisoquinoline-2-carbonyl)pyrrolidine-1-carboxylate (25d). White powder, 52% yield. Mp: 140−142 °C. ^{1}H NMR (DMSO-d_6) δ 1.31 + 1.37 (s, 9H, cis/trans), 1.77−1.94 (m, 4H), 2.24−2.36 (m, 2H), 2.97−3.19 (m, 2H), 3.70 (s, 3H), 4.40 (s, 2H), 4.55−4.92 (m, 4H), 6.78−6.86 (m, 3H), 6.93−6.97 (m, 1H), 7.11−7.27 (m, 1H), 7.38−7.49 (m, 2H), 8.96 (s, 1H), 9.88 (s, 1H), 10.82 (s, 1H). HRMS (AP-ESI) m/z calcd for $C_{29}H_{36}N_4NaO_8$ $[M + Na]^+$ 591.2431, found 591.2448. Retention time: 3.9 min.

***tert*-Butyl (2*S*,3*S*)-1-((*S*)-7-(2-(Hydroxyamino)-2-oxoethoxy)-3-(4-methoxyphenylcarbamoyl)-3,4-dihydroisoquinolin-2(1*H*)-yl)-3-methyl-1-oxopentan-2-ylcarbamate (25e).** White powder, 58% yield. Mp: 138−140 °C. ^{1}H NMR (DMSO-d_6) δ 0.85 (t, J = 7.2 Hz, 3H), 0.91 (d, J = 6.6 Hz, 3H), 1.13−1.17 (m, 1H), 1.24 + 1.36 (s, 9H, cis/trans), 1.48−1.54 (m, 1H), 1.73−1.82 (m, 1H), 2.98−3.13 (m, 2H), 3.70 (s, 3H), 4.45 (s, 2H), 4.65 (d, J = 15.6 Hz, 1H), 4.83−4.86 (m, 1H), 5.01 (d, J = 15.6 Hz, 1H), 5.03−5.06 (m, 1H), 6.75−6.95 (m, 4H), 7.10−7.28 (m, 2H), 7.41−7.44 (m, 2H), 8.97 (s, 1H), 9.87 (s, 1H), 10.82 (s, 1H). HRMS (AP-ESI) m/z calcd for $C_{30}H_{40}N_4NaO_8$ [M + Na]$^+$ 607.2744, found 607.2765. Retention time: 4.1 min.

***tert*-Butyl (*S*)-1-((*S*)-7-(2-(Hydroxyamino)-2-oxoethoxy)-3-(4-methoxyphenylcarbamoyl)-3,4-dihydroisoquinolin-2(1*H*)-yl)-4-methyl-1-oxopentan-2-ylcarbamate (25f).** White powder, 52% yield. Mp: 118−120 °C. ^{1}H NMR (DMSO-d_6) δ 0.93 (d, J = 6.6 Hz, 3H), 0.99 (d, J = 6.6 Hz, 3H), 1.31 + 1.36 (s, 9H, cis/trans), 1.45−1.53 (m, 2H), 1.59−1.70 (m, 1H), 3.02 (dd, J = 15.0 Hz, 6.6 Hz, 1H), 3.13 (dd, J = 15.6 Hz, 6.0 Hz, 1H), 3.70 (s, 3H), 4.41 (s, 2H), 4.56−4.97 (m, 4H), 6.75−6.91 (m, 4H), 7.02−7.25 (m, 2H), 7.40−7.44 (m, 2H), 8.97 (s, 1H), 9.85 (s, 1H), 10.82 (s, 1H). HRMS (AP-ESI) m/z calcd for $C_{30}H_{40}N_4NaO_8$ [M + Na]$^+$ 607.2744, found 607.2764. Retention time: 4.7 min.

***tert*-Butyl (*S*)-1-((*S*)-7-(2-(Hydroxyamino)-2-oxoethoxy)-3-(4-methoxyphenylcarbamoyl)-3,4-dihydroisoquinolin-2(1*H*)-yl)-1-oxopropan-2-ylcarbamate (25g).** White powder, 55% yield. Mp: 181−183 °C. ^{1}H NMR (DMSO-d_6) δ 1.19 (d, J = 6.6 Hz, 3H), 1.24 + 1.35 (s, 9H, cis/trans), 3.01 (dd, J = 15.6 Hz, 6.6 Hz, 1H), 3.12 (dd, J = 15.6 Hz, 6.0 Hz, 1H), 3.70 (s, 3H), 4.41 (s, 2H), 4.54−5.00 (m, 4H), 6.75−6.85 (m, 3H), 6.91−6.93 (m, 1H), 7.03−7.17 (m, 2H), 7.29−7.46 (m, 2H), 8.97 (s, 1H), 9.82 (s, 1H), 10.82 (s, 1H). HRMS (AP-ESI) m/z calcd for $C_{27}H_{34}N_4NaO_8$ [M + Na]$^+$ 565.2274, found 565.2297. Retention time: 2.4 min.

***tert*-Butyl (*S*)-1-((*S*)-7-(2-(Hydroxyamino)-2-oxoethoxy)-3-(4-methoxyphenylcarbamoyl)-3,4-dihydroisoquinolin-2(1*H*)-yl)-3-methyl-1-oxobutan-2-ylcarbamate (25h).** White powder, 58% yield. Mp: 143−145 °C. ^{1}H NMR (DMSO-d_6) δ 0.86 (d, J = 6.6 Hz, 3H), 0.86 (d, J = 6.6 Hz, 3H), 1.26 + 1.36 (s, 9H, cis/trans), 1.22−1.24 (m, 1H), 3.01 (dd, J = 14.4 Hz, 6.6 Hz, 1H), 3.11 (dd, J = 14.4 Hz, 6.0 Hz, 1H), 3.70 (s, 3H), 4.36- 4.41 (m, 1H), 4.42 (s, 2H), 4.64 (d, J = 15.0 Hz, 1H), 4.80−4.82 (m, 1H), 4.96 (d, J = 15.0 Hz, 1H), 6.75−6.86 (m, 4H), 6.94−6.7.21 (m, 2H), 7.41−7.45 (m, 2H), 8.97 (s, 1H), 9.87 (s, 1H), 10.82 (s, 1H). HRMS (AP-ESI) m/z calcd for $C_{29}H_{38}N_4NaO_8$ [M + Na]$^+$ 593.2587, found 593.2640. Retention time: 3.6 min.

(*S*)-7-(2-(Hydroxyamino)-2-oxoethoxy)-*N*-(4-methoxyphenyl)-2-(2-phenylacetyl)-1,2,3,4-tetrahydroisoquinoline-3-carboxamide (25i). White powder, 59% yield. Mp: 141−143 °C. ^{1}H NMR (DMSO-d_6) δ 3.07−3.17 (m, 2H), 3.70 (s, 3H), 3.91 (s, 2H), 4.41 (s, 2H), 4.68 (d, J = 15.6 Hz, 1H), 4.81 (d, J = 15.6 Hz, 1H), 4.94−4.98 (m, 1H), 6.74−6.85 (m, 2H), 7.07−7.14 (m, 1H), 7.20−7.32 (m, 7H), 7.36−7.40 (m, 2H), 8.96 (s, 1H), 9.80 (s, 1H), 10.82 (s, 1H). HRMS (AP-ESI) m/z calcd for $C_{27}H_{28}N_3O_6$ [M + H]$^+$ 490.1978, found 490.1941. Retention time: 2.2 min.

(*S*)-2-Benzoyl-7-(2-(hydroxyamino)-2-oxoethoxy)-*N*-(4-methoxyphenyl)-1,2,3,4-tetrahydroisoquinoline-3-carboxamide (25j). White powder, 53% yield. Mp: 133−135 °C. ^{1}H NMR (DMSO-d_6) δ 3.08−3.26 (m, 2H), 3.70 (s, 3H), 4.42 (s, 2H), 4.51 (d, J = 15.6 Hz, 1H), 4.59 (d, J = 15.6 Hz, 1H), 4.95−5.00 (m, 1H), 6.75−6.90 (m, 2H), 7.07−7.19 (m, 1H), 7.27−7.52 (m, 9H), 8.95 (s, 1H), 10.00 (s, 1H), 10.76 (s, 1H). HRMS (AP-ESI) m/z calcd for $C_{26}H_{26}N_3O_6$ [M + H]$^+$ 476.1822, found 476.1829. Retention time: 2.0 min.

(*S*)-7-(2-(Hydroxyamino)-2-oxoethoxy)-*N*-(4-methoxyphenyl)-2-(4-phenylbutanoyl)-1,2,3,4-tetrahydroisoquinoline-3-carboxamide (25k). White powder, 52% yield. Mp: 140−142 °C. ^{1}H NMR (DMSO-d_6) δ 1.80−1.87 (m, 2H), 2.54−2.58 (m, 2H), 2.62−2.67 (m, 2H), 3.10−3.22 (m, 4H), 3.70 (s, 3H), 4.44 (s, 2H), 4.59−5.05 (m, 3H), 6.75−6.86 (m, 4H), 7.10−7.23 (m, 5H), 7.28−7.40 (m, 3H), 8.96 (s, 1H), 9.74 (s, 1H), 10.82 (s, 1H). HRMS (AP-ESI) m/z calcd for $C_{29}H_{31}N_3NaO_6$ [M + Na]$^+$ 540.2111, found 540.2134. Retention time: 3.2 min.

(*S*)-7-(2-(Hydroxyamino)-2-oxoethoxy)-*N*-(4-methoxyphenyl)-2-(3-phenylpropyl)-1,2,3,4-tetrahydroisoquinoline-3-carboxamide (25l). White powder, 57% yield. Mp: 110−112 °C. ^{1}H NMR (DMSO-d_6) δ 1.83−1.86 (m, 2H), 2.59−2.61 (m, 4H), 2.91−2.94 (m, 2H), 3.51−3.53 (m, 1H), 3.68 (d, J = 15.6 Hz, 1H), 3.71 (s, 3H), 4.03 (d, J = 15.6 Hz, 1H), 4.40 (s, 2H), 6.72−6.75 (m, 2H), 6.86 (d, J = 9.0 Hz, 2H), 7.05−7.06 (m, 1H), 7.13−7.25 (m, 5H), 7.50 (d, J = 9.0 Hz, 2H), 8.96 (s, 1H), 9.75 (s, 1H), 10.80 (s, 1H). HRMS (AP-ESI) m/z calcd for $C_{28}H_{32}N_3O_5$ [M + H]$^+$ 490.2342, found 490.2506. Retention time: 1.6 min.

(*S*)-7-(2-(Hydroxyamino)-2-oxoethoxy)-*N*-(4-methoxyphenyl)-2-phenethyl-1,2,3,4-tetrahydroisoquinoline-3-carboxamide (25m). White powder, 56% yield. Mp: 96−98 °C. ^{1}H NMR (DMSO-d_6) δ 2.76−2.86 (m, 4H), 2.90−2.94 (m, 2H), 3.58−3.60 (m, 1H), 3.70 (s, 3H), 3.79 (d, J = 15.6 Hz, 1H), 4.07 (d, J = 15.6 Hz, 1H), 4.41 (s, 2H), 6.74−6.76 (m, 2H), 6.84 (d, J = 9.0 Hz, 2H), 7.05−7.07 (m, 1H), 7.16−7.27 (m, 5H), 7.38 (d, J = 9.0 Hz, 2H), 8.96 (s, 1H), 9.56 (s, 1H), 10.81 (s, 1H). HRMS (AP-ESI) m/z calcd for $C_{27}H_{30}N_3O_5$ [M + H]$^+$ 476.2185, found 476.2145. Retention time: 1.6 min.

(*S*)-2-Benzyl-7-(2-(hydroxyamino)-2-oxoethoxy)-*N*-(4-methoxyphenyl)-1,2,3,4-tetrahydroisoquinoline-3-carboxamide (25n). White powder, 53% yield. Mp: 90−92 °C. ^{1}H NMR (DMSO-d_6) δ 2.96−3.05 (m, 2H), 3.60−3.66 (m, 3H), 3.71 (s, 3H), 3.76−3.88 (m, 2H), 4.38 (s, 2H), 6.61 (d, J = 2.4 Hz, 1H), 6.75 (dd, J = 2.4 Hz, J = 8.4 Hz, 1H), 6.87 (d, J = 7.2 Hz, 2H), 7.08 (d, J = 8.4 Hz, 1H), 7.27 (t, J = 7.2 Hz, 1H), 7.34 (d, J = 7.2 Hz, 2H), 7.41 (d, J = 7.2 Hz, 2H), 7.53 (d, J = 7.2 Hz, 2H), 8.94 (s, 1H), 9.87 (s, 1H), 10.77 (s, 1H). HRMS (AP-ESI) m/z calcd for $C_{26}H_{27}N_3NaO_5$ [M + Na]$^+$ 484.1848, found 484.1840. Retention time: 1.5 min.

(*S*)-*tert*-Butyl 2-((2*S*,3*S*)-1-((*S*)-7-(2-(Hydroxyamino)-2-oxoethoxy)-3-(4-methoxyphenylcarbamoyl)-3,4-dihydroisoquinolin-2(1*H*)-yl)-3-methyl-1-oxopentan-2-ylcarbamoyl)-pyrrolidine-1-carboxylate (30a). White powder, 52% yield. Mp: 129−131 °C. ^{1}H NMR (DMSO-d_6) δ 0.72−0.94 (m, 6H), 1.02−1.43 (m, 11H), 1.55−1.88 (m, 4H), 2.06−2.13 (m, 1H), 2.97−3.35 (m, 4H), 3.70 (s, 3H), 4.14−4.27 (m, 1H), 4.44 (s, 2H), 4.53−4.70 (m, 1H), 4.73−4.87 (m, 2H), 4.91−5.16 (m, 1H), 6.73−6.87 (m, 4H), 7.02−7.12 (m, 1H), 7.34−7.52 (m, 2H), 7.94−8.43 (m, 1H), 8.96 (s, 1H), 9.43−10.07 (m, 1H), 10.81 (s, 1H). HRMS (AP-ESI) m/z calcd for $C_{35}H_{47}N_5NaO_9$ [M + Na]$^+$ 704.3363, found 704.3271. Retention time: 3.8 min.

***tert*-Butyl (*S*)-1-((2*S*,3*S*)-1-((*S*)-7-(2-(Hydroxyamino)-2-oxoethoxy)-3-(4-methoxyphenylcarbamoyl)-3,4-dihydroisoquinolin-2(1*H*)-yl)-3-methyl-1-oxopentan-2-ylamino)-3-methyl-1-oxobutan-2-ylcarbamate (30b, 57% yield).** White powder. Mp: 131−133 °C. ^{1}H NMR (DMSO-d_6) δ 0.72−0.98 (m, 12H), 1.11−1.19 (m, 1H), 1.21−1.32 (m, 1H), 1.33 + 1.37 (s, 9H, cis/trans), 1.69−1.79 (m, 1H), 1.81−1.92 (m, 1H), 2.98−3.25 (m, 2H), 3.69 (s, 3H), 3.77−3.97 (m, 1H), 4.40 (s, 2H), 4.51−5.10 (m, 4H), 6.61−6.92 (m, 4H), 7.06−7.15 (m, 1H), 7.33−7.53 (m, 2H), 7.89 (s, 1H), 8.06 (s, 1H), 8.95 (s, 1H), 9.87 (s, 1H), 10.81 (s, 1H). HRMS (AP-ESI) m/z calcd for $C_{35}H_{50}N_5O_9$ [M + H]$^+$ 684.3609, found 684.3629. Retention time: 5.0 min.

***tert*-Butyl 4-((2*S*,3*S*)-1-((*S*)-7-(2-(Hydroxyamino)-2-oxoethoxy)-3-(4-methoxyphenylcarbamoyl)-3,4-dihydroisoquinolin-2(1*H*)-yl)-3-methyl-1-oxopentan-2-ylcarbamoyl)-piperidine-1-carboxylate (30c).** White powder, 55% yield. Mp: 135−137 °C. ^{1}H NMR (DMSO-d_6) δ 0.80−0.96 (m, 6H), 1.09−1.16 (m, 1H), 1.30−1.38 (m, 1H), 1.39 (s, 9H), 1.49−1.59 (m, 2H),

1.68−1.71 (m, 2H), 1.72−1.80 (m, 1H), 2.37−2.55 (m, 1H), 2.58−2.77 (m, 2H), 2.97−3.26 (m, 2H), 3.68 (s, 3H), 3.84−4.00 (m, 2H), 4.40 (s, 2H), 4.50−5.10 (m, 4H), 6.73−6.93 (m, 4H), 7.07−7.16 (m, 1H), 7.34−7.50 (m, 2H), 8.23 (s, 1H), 9.24 (s, 1H), 9.85 (s, 1H), 10.81 (s, 1H). HRMS (AP-ESI) m/z calcd for $C_{36}H_{50}N_5O_9$ $[M + H]^+$ 696.3609, found 696.3634. Retention time: 4.1 min.

***tert*-Butyl (2*S*,3*S*)-1-((*S*)-7-(2-(Hydroxyamino)-2-oxoethoxy)-3-(4-methoxyphenylcarbamoyl)-3,4-dihydroisoquinolin-2(1*H*)-yl)-3-methylpentan-2-ylcarbamate (34a).** White powder, 58% yield. Mp: 98−100 °C. ^{1}H NMR (DMSO-d_6) δ 0.80−0.89 (m, 6H), 1.03−1.07 (m, 1H), 1.34 + 1.36 (s, 9H, cis/trans), 1.38−1.39 (m, 1H), 1.42−1.51 (m, 1H), 2.42−2.46 (m, 1H), 2.68−2.70 (m, 1H), 2.91−2.99 (m, 2H), 3.59−3.61 (m, 2H), 3.66−3.69 (m, 1H), 3.70 (s, 3H), 3.98−4.00 (m, 1H), 4.40 (s, 2H), 6.59−6.79 (m, 3H), 6.84−6.86 (m, 2H), 7.03−7.06 (m, 1H), 7.49−7.53 (m, 2H), 8.95 (s, 1H), 9.67 (s, 1H), 10.79 (s, 1H). HRMS (AP-ESI) m/z calcd for $C_{30}H_{42}N_4NaO_7$ $[M + Na]^+$ 593.2951, found 593.2978. Retention time: 2.6 min.

(*S*)-2-((2*S*,3*S*)-2-(3,3-Dimethylbutanamido)-3-methylpentyl)-7-(2-(hydroxyamino)-2-oxoethoxy)-*N*-(4-methoxyphenyl)-1,2,3,4-tetrahydroisoquinoline-3-carboxamide (34b). White powder, 55% yield. Mp: 119−121 °C. ^{1}H NMR (DMSO-d_6) δ 0.75−0.85 (m, 6H), 0.94−0.96 (m, 9H), 1.02−1.10 (m, 1H), 1.23−1.43 (m, 1H), 1.52−1.57 (m, 1H), 1.91−2.09 (m, 2H), 2.37−2.77 (m, 2H), 2.85−3.01 (m, 2H), 3.58−3.95 (m, 2H), 3.70 (s, 3H), 3.98−4.00 (m, 1H), 4.10−4.12 (m, 1H), 4.40 (s, 2H), 6.64−6.87 (m, 4H), 7.04−7.05 (m, 1H), 7.39−7.58 (m, 3H), 8.96 (s, 1H), 9.74 (s, 1H), 10.80 (s, 1H). HRMS (AP-ESI) m/z calcd for $C_{31}H_{45}N_4O_6$ $[M + H]^+$ 569.3339, found 569.3681. Retention time: 2.5 min.

General Procedure for the Preparation of 26a and Its Analogues 26b−26h, 31a−31c (*S*)-2-(2-Aminoacetyl)-7-(2-(hydroxyamino)-2-oxoethoxy)-*N*-(4-methoxyphenyl)-1,2,3,4-tetrahydroisoquinoline-3-carboxamide Hydrochloride (26a). To a solution of compound **25a** (0.26 g, 0.5 mmol) in dry EtOAc (8 mL) was added a solution of EtOAc (8 mL) saturated by dry HCl gas. The reaction solution was stirred at room temperature for 3 h at which time a precipitate appeared. The suspension was filtered, with the filter being washed with ether, to give desired compound **26a** (0.21 g, 90% yield) as a white powder. Mp: 193−195 °C. ^{1}H NMR (DMSO-d_6) δ 3.12−3.14 (m, 2H), 3.70 (s, 3H), 4.08−4.09 (m, 2H), 4.42 (s, 2H), 4.65−4.70 (m, 2H), 5.00−5.01 (m, 1H), 6.80−6.90 (m, 4H), 7.15−7.16 (m, 1H), 7.37−7.42 (m, 2H), 8.19 (br s, 3H), 8.98 (br s, 1H), 9.90 (s, 1H), 10.86 (s, 1H). HRMS (AP-ESI) m/z calcd for $C_{21}H_{24}N_4NaO_6$ $[M + Na]^+$ 451.1594, found 451.1600. Retention time: 1.9 min.

(*S*)-2-((*S*)-2-Amino-3-phenylpropanoyl)-7-(2-(hydroxyamino)-2-oxoethoxy)-*N*-(4-methoxyphenyl)-1,2,3,4-tetrahydroisoquinoline-3-carboxamide Hydrochloride (26b). White powder, 91% yield. Mp: 188−190 °C. ^{1}H NMR (DMSO-d_6) δ 2.99−3.08 (m, 2H), 3.13−3.24 (m, 2H), 3.72 (s, 3H), 4.45 (s, 2H), 4.65−4.90 (m, 4H), 6.72−6.98 (m, 4H), 7.19−7.34 (m, 5H), 7.40−7.51 (m, 3H), 8.45 (br s, 3H), 8.96 (br s, 1H), 10.09 (s, 1H), 10.83 (s, 1H). HRMS (AP-ESI) m/z calcd for $C_{28}H_{31}N_4O_6$ $[M + H]^+$ 519.2244, found 519.2287. Retention time: 5.9 min.

(*S*)-2-((*S*)-2-Amino-3-(4-hydroxyphenyl)propanoyl)-7-(2-(hydroxyamino)-2-oxoethoxy)-*N*-(4-methoxyphenyl)-1,2,3,4-tetrahydroisoquinoline-3-carboxamide Hydrochloride (26c). White powder, 92% yield. Mp: 180−182 °C. ^{1}H NMR (DMSO-d_6) δ 2.87−3.05 (m, 2H), 3.06−3.21 (m, 2H), 3.72 (s, 3H), 4.45 (s, 2H), 4.51−4.90 (m, 4H), 6.66−6.90 (m, 5H), 7.00−7.24 (m, 4H), 7.39−7.50 (m, 2H), 8.19 (br s, 3H), 8.97 (br s, 1H), 9.39 (s, 1H), 10.10 (s, 1H), 10.85 (s, 1H). HRMS (AP-ESI) m/z calcd for $C_{28}H_{31}N_4O_7$ $[M + H]^+$ 535.2193, found 535.2262. Retention time: 3.0 min.

(*S*)-7-(2-(Hydroxyamino)-2-oxoethoxy)-*N*-(4-methoxyphenyl)-2-((*S*)-pyrrolidine-2-carbonyl)-1,2,3,4-tetrahydroisoquinoline-3-carboxamide Hydrochloride (26d). White powder, 88% yield. Mp: 190−192 °C. ^{1}H NMR (DMSO-d_6) δ 1.89−2.00 (m, 4H), 3.02−3.26 (m, 4H), 3.70 (s, 3H), 4.42 (s, 2H), 4.50−5.06 (m, 4H), 6.83−6.87 (m, 3H), 6.99−7.00 (m, 1H), 7.20−7.21 (m, 1H), 7.40−7.46 (m, 2H), 8.65 (br s, 2H), 9.71 (br s, 1H), 10.22 (s, 1H), 10.87 (s, 1H). HRMS (AP-ESI) m/z calcd for $C_{24}H_{29}N_4O_6$ $[M + H]^+$ 469.2087, found 469.2153. Retention time: 2.7 min.

(*S*)-2-((2*S*,3*S*)-2-Amino-3-methylpentanoyl)-7-(2-(hydroxyamino)-2-oxoethoxy)-*N*-(4-methoxyphenyl)-1,2,3,4-tetrahydroisoquinoline-3-carboxamide Hydrochloride (26e). White powder, 91% yield. Mp: 176−178 °C. ^{1}H NMR (DMSO-d_6) δ 0.85 (t, J = 7.2 Hz, 3H), 1.08 (d, J = 6.6 Hz, 3H), 1.18−1.22 (m, 1H), 1.58−1.62 (m, 1H), 1.91−1.96 (m, 1H), 3.03 (dd, J = 15.6 Hz, 8.4 Hz, 1H), 3.18 (dd, J = 15.6 Hz, 6.0 Hz, 1H), 3.71 (s, 3H), 4.42 (s, 2H), 4.53−4.98 (m, 4H), 6.83−6.88 (m, 3H), 7.04−7.05 (m, 1H), 7.20−7.21 (m, 1H), 7.44−7.46 (m, 2H), 8.08 (s, 3H), 8.98 (br s, 1H), 10.07 (s, 1H), 10.88 (s, 1H). HRMS (AP-ESI) m/z calcd for $C_{25}H_{33}N_4O_6$ $[M + H]^+$ 485.2400, found 485.2594. Retention time: 4.8 min.

(*S*)-2-((*S*)-2-Amino-4-methylpentanoyl)-7-(2-(hydroxyamino)-2-oxoethoxy)-*N*-(4-methoxyphenyl)-1,2,3,4-tetrahydroisoquinoline-3-carboxamide Hydrochloride (26f). White powder, 93% yield. Mp: 168−170 °C. ^{1}H NMR (DMSO-d_6) δ 0.95 (d, J = 6.6 Hz, 3H), 1.08 (d, J = 6.6 Hz, 3H), 1.60−1.71 (m, 2H), 1.89−1.91 (m, 1H), 3.06 (dd, J = 15.0 Hz, 7.2 Hz, 1H), 3.18 (dd, J = 15.6 Hz, 6.0 Hz, 1H), 3.70 (s, 3H), 4.42 (s, 2H), 4.55−4.87 (m, 4H), 6.83−6.86 (m, 3H), 7.03−7.05 (m, 1H), 7.19−7.20 (m, 1H), 7.44−7.47 (m, 2H), 8.22 (s, 3H), 8.96 (s, 1H), 10.11 (s, 1H), 10.88 (s, 1H). HRMS (AP-ESI) m/z calcd for $C_{25}H_{33}N_4O_6$ $[M + H]^+$ 485.2400, found 485.2468. Retention time: 4.5 min.

(*S*)-2-((*S*)-2-Aminopropanoyl)-7-(2-(hydroxyamino)-2-oxoethoxy)-*N*-(4-methoxyphenyl)-1,2,3,4-tetrahydroisoquinoline-3-carboxamide Hydrochloride (26g). White powder, 90% yield. Mp: 194−196 °C. ^{1}H NMR (DMSO-d_6) δ 1.44 (d, J = 6.6 Hz, 3H), 3.01 (dd, J = 14.4 Hz, 8.4 Hz, 1H), 3.20 (dd, J = 14.4 Hz, 6.0 Hz, 1H), 3.71 (s, 3H), 4.42 (s, 2H), 4.45−4.89 (m, 4H), 6.83−6.87 (m, 3H), 6.98−7.01 (m, 1H), 7.20−7.22 (m, 1H), 7.42−7.48 (m, 2H), 8.15 (s, 3H), 8.96 (br s, 1H), 10.06 (s, 1H), 10.83 (s, 1H). HRMS (AP-ESI) m/z calcd for $C_{22}H_{27}N_4O_6$ $[M + H]^+$ 443.1931, found 443.1954. Retention time: 2.3 min.

(*S*)-2-((*S*)-2-Amino-3-methylbutanoyl)-7-(2-(hydroxyamino)-2-oxoethoxy)-*N*-(4-methoxyphenyl)-1,2,3,4-tetrahydroisoquinoline-3-carboxamide Hydrochloride (26h). White powder, 91% yield. Mp: 178−180 °C. ^{1}H NMR (DMSO-d_6) δ 0.93 (d, J = 6.6 Hz, 3H), 1.01 (d, J = 6.6 Hz, 3H), 2.23−2.26 (m, 1H), 3.02 (dd, J = 15.0 Hz, 9.0 Hz, 1H), 3.20 (dd, J = 15.0 Hz, 6.0 Hz, 1H), 3.71 (s, 3H), 4.41−4.52 (m, 1H), 4.42 (s, 2H), 4.54 (d, J = 15.0 Hz, 1H), 4.68−4.70 (m, 1H), 4.97 (d, J = 15.0 Hz, 1H), 6.84−6.88 (m, 3H), 7.04−7.05 (m, 1H), 7.20−7.22 (m, 1H), 7.45−7.47 (m, 2H), 8.09 (s, 3H), 8.99 (br s, 1H), 10.10 (s, 1H), 10.88 (s, 1H). HRMS (AP-ESI) m/z calcd for $C_{24}H_{31}N_4O_6$ $[M + H]^+$ 471.2244, found 471.2271. Retention time: 3.4 min.

(*S*)-7-(2-(Hydroxyamino)-2-oxoethoxy)-*N*-(4-methoxyphenyl)-2-((2*S*,3*S*)-3-methyl-2-((*S*)-pyrrolidine-2-carboxamido)-pentanoyl)-1,2,3,4-tetrahydroisoquinoline-3-carboxamide Hydrochloride (31a). White powder, 93% yield. Mp: 173−175 °C. ^{1}H NMR (DMSO-d_6) δ 0.73−0.99 (m, 6H), 1.06−1.19 (m, 1H), 1.26−1.34 (m, 1H), 1.71−1.84 (m, 2H), 1.85−1.95 (m, 2H), 2.20−2.39 (m, 1H), 3.02−3.29 (m, 4H), 3.70 (s, 3H), 4.20−4.31 (m, 1H), 4.44 (s, 2H), 4.54−4.69 (m, 1H), 4.72−4.88 (m, 2H), 4.90−5.10 (m, 1H), 6.74−6.97 (m, 4H), 7.09−7.20 (m, 1H), 7.35−7.47 (m, 2H), 8.49−8.55 (m, 1H), 8.74−8.89 (m, 1H), 8.98 (br s, 1H), 9.95 (s, 1H), 10.02−10.35 (m, 1H), 10.89 (s, 1H). HRMS (AP-ESI) m/z calcd for $C_{30}H_{40}N_5O_7$ $[M + H]^+$ 582.2928, found 582.2972. Retention time: 5.1 min.

(*S*)-2-((2*S*,3*S*)-2-((*S*)-2-Amino-3-methylbutanamido)-3-methylpentanoyl)-7-(2-(hydroxyamino)-2-oxoethoxy)-*N*-(4-methoxyphenyl)-1,2,3,4-tetrahydroisoquinoline-3-carboxamide Hydrochloride (31b). White powder, 88% yield. Mp: 176−178 °C.

^{1}H NMR (DMSO-d_6) δ 0.74−1.02 (m, 12H), 1.13−1.18 (m, 1H), 1.27−1.65 (m, 1H), 1.70−1.88 (m, 1H), 1.95−2.16 (m, 1H), 3.01−3.29 (m, 2H), 3.64−3.87 (m, 1H), 3.70 (s, 3H), 4.44 (s, 2H), 4.54−5.30 (m, 4H), 6.75−6.96 (m, 4H), 7.10−7.19 (m, 1H), 7.35−7.48 (m, 2H), 8.18 (s, 3H), 8.63 (s, 1H), 8.98 (s, 1H), 9.96 (s, 1H), 10.87 (s, 1H). HRMS (AP-ESI) m/z calcd for $C_{30}H_{42}N_5O_7$ $[M + H]^+$ 584.3084, found 584.3158. Retention time: 7.5 min.

(*S*)-7-(2-(Hydroxyamino)-2-oxoethoxy)-*N*-(4-methoxyphenyl)-2-((2*S*,3*S*)-3-methyl-2-(piperidine-4-carboxamido) pentanoyl)-1,2,3,4-tetrahydroisoquinoline-3-carboxamide Hydrochloride (31c). White powder, 92% yield. Mp: 180−182 °C. ^{1}H NMR (DMSO-d_6) δ 0.81−0.96 (m, 6H), 1.09−1.17 (m, 1H), 1.28−1.33 (m, 1H), 1.68−1.80 (m, 4H), 1.86−1.91 (m, 1H), 2.52−2.65 (m, 1H), 2.58−2.78 (m, 2H), 3.00−3.18 (m, 2H), 3.21−3.29 (m, 2H), 3.70 (s, 3H), 4.28−5.05 (m, 4H), 4.43 (s, 2H), 6.75−7.01 (m, 4H), 7.11−7.21 (m, 1H), 7.43−7.57 (m, 2H), 8.26 (s, 1H), 8.56 (s, 2H), 9.38 (s, 1H), 9.84 (s, 1H), 10.89 (s, 1H). HRMS (AP-ESI) m/z calcd for $C_{31}H_{42}N_5O_7$ $[M + H]^+$ 596.3084, found 596.3181. Retention time: 4.2 min.

In Vitro HDAC Inhibition Fluorescence Assay. In vitro activity against HDAC8 was determined as previously described.[24] Briefly, HDAC8 solution (10 μL) was mixed with various concentrations of compound sample (50 μL). Fluorogenic substrate (40 μL) was added, and the mixture was incubated at 37 °C for 30 min and then stopped by addition of 100 μL of developer containing trypsin and TSA. Fluorescence intensity was measured after 20 min using a microplate reader at excitation and emission wavelengths of 390 and 460 nm, respectively. The inhibition ratios were calculated from the fluorescence intensity readings of tested wells relative to those of control wells, and the IC_{50} values were determined using a regression analysis of the concentration/inhibition data. The procedures of HeLa nuclear extract assay and HDAC6 (purchased from abcam Ltd.) assay were similar to that of HDAC8.

In Vitro Antiproliferative Assay. All cell lines were maintained in RPMI1640 medium containing 10% FBS at 37 °C in a 5% CO_2 humidified incubator. Cell proliferation assay was determined by the MTT (3-[4,5-dimethyl-2-thiazolyl]-2,5-diphenyl-2*H*-tetrazolium bromide) method. Briefly, cells were passaged the day before dosing into a 96-well cell plate, allowed to grow for a minimum of 4 h, and then treated with different concentrations of compound sample for 48 h. A 0.5% MTT solution was added to each well. After further incubation for another 4 h, formazan formed from MTT was extracted by adding 200 μL of DMSO for 15 min. Absorbance was then determined using an ELISA reader at 570 nm.

In Vivo Antitumor Assay against MDA-MB-231 Xenograft. For in vivo antitumor efficacy research, 5×10^6 human breast cancer cells (MDA-MB-231) were inoculated subcutaneously in the right flank of female athymic nude mice (5−6 weeks old, Slac Laboratory Animal, Shanghai). Ten days after injection, tumors were palpable and mice were randomized into treatment and control groups (six mice per group). The treatment groups received 90 mg/kg/d compounds intraperitoneally (i.p.), and the blank control group received an equal volume of PBS solution containing 40% DMSO intraperitoneally. During treatment, subcutaneous tumors were measured with a vernier caliper every three days, and body weight was monitored regularly. Tumor volumes (V) were estimated using the equation ($V = ab^2/2$, where a and b stand for the longest and shortest diameter, respectively). Relative increment ratio (T/C) was calculated according to the following formula:

$$\text{T/C (\%)} = \text{the treatment group (T) RTV} / \text{the blank control group (C) RTV}$$

where RTV, namely relative tumor volume = V_t/V_0 (V_t: the tumor volume measured at the end of treatment; V_0: the tumor volume measured at the beginning of randomization).

Molecular Docking Studies. Compounds were docked into the active site of HDAC8 (PDB entry: 1T64) using Tripos SYBYL 8.0. The residues in a radius of 12.0 Å around TSA in the cocrystal structure of HDAC8 and TSA (PDB entry: 1T64) were selected as the active site. Before the docking process, the protein structure was treated by deleting water molecules, adding hydrogen atoms, modifying atom types, and assigning AMBER7 FF99 charge. A 100-step minimization process was performed to further optimize the protein structure. The molecular structures were generated with the Sybyl/Sketch module and optimized using Powell's method with the Tripos force field with convergence criterion set at 0.05 kcal/(Å mol) and assigned with the Gasteiger−Hückel method. Molecular docking was carried out via the Sybyl/FlexX module. Other docking parameters implied in the program were default values.

■ ASSOCIATED CONTENT

Supporting Information. ^{1}H NMR spectral information of the key intermediate **23**, representative target compounds **22a**, **22b**, **25c**, **25e**, **25f**, **25h**, **25l**, **25m**, **25n**, **26a**, **26e**, **26f**, **26h**, **34a**, and **34b**. HPLC analysis chromatograms of representative target compounds **22a**, **22b**, **25c**, **25e**, **25f**, **25h**, **25l**, **25m**, **25n**, **26a**, **26e**, **26f**, **26h**, **34a**, and **34b**. This material is available free of charge via the Internet at http://pubs.acs.org.

■ AUTHOR INFORMATION

Corresponding Author

*Phone: 86-531-88382264. Fax: 86-531-88382264. E-mail: wfxu@yahoo.cn or haofangcn@sdu.edu.cn.

■ ACKNOWLEDGMENT

This work was supported by National Nature Science Foundation of China (Grant No. 30772654 and No. 90713041) and National High Technology Research and Development Program of China (863 project; Grant No. 2007AA02Z314) and National Science and Technology Major Project (Grant No. 2009-ZX09103-118).

■ ABBREVIATIONS:

HDAC, histone deacetylase; HDACi, histone deacetylase inhibitors; SAR, structure−activity relationships; SAHA, suberoylanilide hydroxamic acid; ZBG, zinc-binding group; Boc, *tert*-butoxycarbonyl

■ REFERENCES

(1) Hassig, C. A.; Schreiber, S. L. Nuclear histone acetylases and deacetylases and transcriptional regulation: HATs off to HDACs. *Curr. Opin. Chem. Biol.* **1997**, *1*, 300–308.

(2) Kouzarides, T. Histone acetylases and deacetylases in cell proliferation. *Curr. Opin. Genet. Dev.* **1999**, *9*, 40–48.

(3) Wolffe, A. P. Histone deacetylase: a regulator of transcription. *Science (Washington, DC, U. S.)* **1996**, *272*, 371–372.

(4) Dokmanovic, M.; Clarke, C.; Marks, P. A. Histone deacetylase inhibitors: overview and perspectives. *Mol. Cancer Res.* **2007**, *5*, 981–989.

(5) Ropero, S.; Esteller, M. The role of histone deacetylases (HDACs) in human cancer. *Mol. Oncol.* **2007**, *1*, 19–25.

(6) de Ruijter, A. J.; van Gennip, A. H.; Caron, H. N.; Kemp, S.; van Kuilenburg, A. B. Histone deacetylases (HDACs): Characterisation of the classical HDAC family. *Biochem. J.* **2003**, *370*, 737–749.

(7) Glozak, M. A.; Sengupta, N.; Zhang, X.; Seto, E. Acetylation and deacetylation of non-histone proteins. *Gene* **2005**, *363*, 15–23.

(8) Halkidou, K.; Gaughan, L.; Cook, S.; Leung, H. Y.; Neal, D. E.; Robson, C. N. Upregulation and nuclear recruitment of HDAC1 in hormone refractory prostate cancer. *Prostate* **2004**, *59*, 177–189.

(9) Choi, J. H.; Kwon, H. J.; Yoon, B.-I.; Kim, J. H.; Han, S. U.; Joo, H. J.; Kim, D.-Y. Expression profile of histone deacetylase1 in gastric cancer tissues. *Jpn. J. Cancer Res.* **2001**, *92*, 1300–1304.

(10) Wilson, A. J.; Byun, D.-S.; Popova, N.; Murray, L. B.; L'Italien, K.; Sowa, Y.; Arango, D.; Velcich, A.; Augenlicht, L. H.; Mariadason, J. M. Histone deacetylase 3 (HDAC3) and other class I HDACs regulate colon cell maturation and p21 expression and are deregulated in human colon cancer. *J. Biol. Chem.* **2006**, *281*, 13548–13558.

(11) Zhang, Z. H.; Yamashita, H.; Toyama, T.; Sugiura, H.; Ando, Y.; Mita, K.; Hamaguchi, M.; Hara, Y.; Kobayashi, S.; Iwase, H. Quantitation of HDAC1 mRNA expression in invasive carcinoma of the breast. *Breast Cancer Res. Treat.* **2005**, *94*, 11–16.

(12) Zhu, P.; Martin, E.; Mengwasser, J.; Schlag, P.; Janssen, K.-P.; Gottlicher, M. Induction of HDAC2 expression upon loss of APC in colorectal tumorigenesis. *Cancer Cell* **2004**, *5*, 455–463.

(13) Huang, B. H.; Laban, M.; Leung, CH-W.; Lee, L.; Lee, C. K.; Salto-Tellez, M.; Raju, G. C.; Hooi, S. C. Inhibition of histone deacetylase 2 increases apoptosis and p21Cip1/WAF1 expression, independent of histone deacetylase 1. *Cell Death Differ.* **2005**, *12* 395–404.

(14) Song, J.; Noh, J. H.; Lee, J. H.; Eun, J. W.; Ahn, Y. M.; Kim, S. Y.; Lee, S. H.; Park, W. S.; Yoo, N . J.; Lee, J. Y.; Nam, S. W. Increased expression of histone deacetylase 2 is found in human gastric cancer. *APMIS* **2005**, *113*, 264–268.

(15) Zhang, Z. H.; Yamashita, H.; Toyama, T.; Sugiura, H.; Omoto, Y.; Ando, Y.; Mita, K.; Hamaguchi, M.; Hayashi, S.-I.; Iwase, H. HDAC6 expression is correlated with better survival in breast cancer. *Clin. Cancer Res.* **2004**, *10*, 6962–6968.

(16) Miller, T. A.; Witter, D. J.; Belvedere, S. Histone deacetylase inhibitors. *J. Med. Chem.* **2003**, *46*, 5097–5116.

(17) Al-Janadi, A.; Chandana., S. R.; Cloney, B. A. Histone deacetylase: an attractive target for cancer therapy. *Drugs R&D* **2008**, *9*, 369–383.

(18) Butler, L. M.; Agus, D. B.; Scher, H. I.; Higgins, B.; Rose, A.; Cordon-Cardo, C.; Thaler, H. T.; Rifkind, R. A.; Marks, P. A.; Richon, V. M. Suberoylanilide hydroxamic acid, an inhibitor of histone deacetylase, suppresses the growth of prostate cancer cells in vitro and in vivo. *Cancer Res.* **2000**, *60*, 5165–5170.

(19) Garber, K. HDAC inhibitors overcome first hurdle. *Nat. Biotechnol.* **2007**, *25*, 17–19.

(20) Grant, S.; Easley, C.; Kirkpatrick, P. Vorinostat. *Nat. Rev. Drug Discovery* **2007**, *6*, 21–22.

(21) Marks, P. A.; Breslow, R. Dimethyl sulfoxide to vorinostat: development of this histone deacetylase inhibitor as an anticancer drug. *Nat. Biotechnol.* **2007**, *25*, 84–90.

(22) Campas-Moya, C. Romidepsin for the treatment of cutaneous T-cell lymphoma. *Drugs Today* **2009**, *45*, 787–795.

(23) Zhang, Y.; Fang, H.; Jiao, J.; Xu, W. The structure and function of histone deacetylases: the target for anti-cancer therapy. *Curr. Med. Chem.* **2008**, *15*, 2840–2849.

(24) Zhang, Y.; Feng, J.; Liu, C.; Zhang, L.; Jiao, J.; Fang, H.; Su, L.; Zhang, X.; Zhang, J.; Li, M.; Wang, B.; Xu, W. Design, synthesis and preliminary activity assay of 1,2,3,4-tetrahydroisoquinoline-3-carboxylic acid derivatives as novel histone deacetylases (HDACs) inhibitors. *Bioorg. Med. Chem.* **2010**, *18*, 1761–1772.

(25) Donkor, I. O.; Zheng, X.; Han, J.; Lacy, C.; Miller, D. D. Significance of hydrogen bonding at the S_1' subsite of calpain I. *Bioorg. Med. Chem. Lett.* **2001**, *11*, 1753–1755.

(26) Fournel, M.; Bonfils, C.; Hou, Y.; Yan, P. T.; Trachy-Bourget, M. C.; Kalita, A.; Liu, J.; Lu, A. H.; Zhou, N. Z.; Robert, M. F.; Gillespie, J.; Wang, J. J.; Ste-Croix, H.; Rahil, J.; Lefebvre, S.; Moradei, O.; Delorme, D.; Macleod, A. R.; Besterman, J. M.; Li, Z. MGCD0103, a novel isotype-selective histone deacetylase inhibitor, has broad spectrum antitumor activity in vitro and in vivo. *Mol. Cancer Ther.* **2008**, *7*, 759–768.

(27) Wilson, I. B.; Harrison, S.; Ginsburg, S. Carbamyl derivatives of acetylcholinesterase. *J. Biol. Chem.* **1961**, *236*, 1498–1500.

(28) O'Brien, R. D.; Hilton, B. D.; Gilmour, L. The reaction of carbamates with cholinesterase. *Mol. Pharmacol.* **1966**, *2*, 593–605.

(29) Balasubramanian, S.; Ramos, J.; Luo, W.; Sirisawad, M.; Verner, E.; Buggy, J. J. A novel histone deacetylase 8 (HDAC8)-specific inhibitor PCI-34051 induces apoptosis in T-cell lymphomas. *Leukemia* **2008**, *22*, 1026–1034.

(30) Pettersen, E. F.; Goddard, T. D.; Huang, C. C.; Couch, G. S.; Greenblatt, D. M.; Meng, E. C.; Ferrin, T. E. UCSF Chimera--a visualization system for exploratory research and analysis. *J. Comput. Chem.* **2004**, *25*, 1605–1612.

(31) Mou, J.; Fang, H.; Liu, Y.; Shang, L.; Wang, Q.; Zhang, L.; Xu, W. Design, synthesis and premary activity assay of bi- or tri- peptide analogues with the scaffold L-arginine as amino-peptidase N/CD13 inhibitors. *Bioorg. Med. Chem.* **2010**, *18*, 887–895.